

# Masked Modeling Duo: Towards a Universal Audio Pre-training Framework

Daisuke Niizumi , Daiki Takeuchi, Yasunori Ohishi , *Member, IEEE*, Noboru Harada , *Senior Member, IEEE*, and Kunio Kashino, *Senior Member, IEEE*

**Abstract**—Self-supervised learning (SSL) using masked prediction has made great strides in general-purpose audio representation. This study proposes Masked Modeling Duo (M2D), an improved masked prediction SSL, which learns by predicting representations of masked input signals that serve as training signals. Unlike conventional methods, M2D obtains a training signal by encoding only the masked part, encouraging the two networks in M2D to model the input. While M2D improves general-purpose audio representations, a specialized representation is essential for real-world applications, such as in industrial and medical domains. The often confidential and proprietary data in such domains is typically limited in size and has a different distribution from that in pre-training datasets. Therefore, we propose M2D for X (M2D-X), which extends M2D to enable the pre-training of specialized representations for an application X. M2D-X learns from M2D and an additional task and inputs background noise. We make the additional task configurable to serve diverse applications, while the background noise helps learn on small data and forms a denoising task that makes representation robust. With these design choices, M2D-X should learn a representation specialized to serve various application needs. Our experiments confirmed that the representations for general-purpose audio, specialized for the highly competitive AudioSet and speech domain, and a small-data medical task achieve top-level performance, demonstrating the potential of using our models as a universal audio pre-training framework. Our code is available online for future studies.

**Index Terms**—Self-supervised learning, masked prediction, audio, general-purpose audio representation, specialization.

## I. INTRODUCTION

SELF-SUPERVISED learning (SSL) methods based on masked prediction have made great strides, enabling pre-training of high-performance models in the natural language processing (NLP) and image domains [1]–[7]. They are pre-trained through the task of predicting masked portions from representations that encode unmasked (visible) portions of the input signal. To better predict the masked portions, the information about the input signal from the unmasked portions should be efficiently encoded into a representation to effectively encourage the modeling of the input signal.

In the speech domain, a number of masked prediction-based speech SSL models have been proposed that perform well on a wide range of speech tasks [8]–[11]. In the audio domain, many SSL models have been proposed that perform effectively

in diverse audio tasks, including environmental sounds and music in addition to speech [12]–[16].

In particular, masked autoencoders (MAE) in the image domain sparked a major trend, followed by a number of MAE-based methods in the audio domain [13]–[16]. MAE masks a large portion (75%) of the input signal and reconstructs the masked portion using an encoded representation of the remaining small amount (25%) of the visible portion. It learns an effective representation by efficiently extracting information from the 25% of the input signal using a vision transformer (ViT) [17]. However, MAE learns from reconstruction errors and is thus considered to optimize the representation indirectly.

We believe that representations can be optimized more effectively by involving them in the loss calculation. Methods [4], [5], [18] that encode the input into a representation and use the masked portion of it as a training signal accomplish this. However, since these methods encode the entire input signal, the resulting training signal representation is not always encouraged to model the input. This is because if both the source (visible) and target (masked) information for prediction is available, it may be easier for the training signal to contaminate the target information than to model the signal.

We hypothesize that encoding only the masked portion of the input signal, rather than the entire signal, would encourage the representation to model the input. For example, consider a heart sound consisting of two elements (S1 and S2) as an input signal, where the entire S1 is masked. In this case, if the representation of the unmasked S2 contains only S2 information, it will be difficult to predict S1, but if the information is modeled as part of the whole heart sound, the prediction will be easy. On the other hand, the masked S1 part representation, which is the training signal, is more likely to match the prediction if it is encoded as part of the whole heart sound.

We propose a new method, Masked Modeling Duo (M2D), that implements our hypothesis by encoding the masked and unmasked portions of the input signal separately, thereby encouraging both representations to model the input signal [Fig. 1(a)]. M2D also facilitates the task of masked prediction since the representation of the masked part, which serves as the training signal, has no direct information overlap with the unmasked part used for prediction. M2D follows other MAE configurations, such as using ViT as the encoder. Although our proposed method is simple, it should provide an improvement over MAE and learn representations more effectively.

Manuscript received December 21, 2021; revised September 18, 2022.

The authors are with Communication Science Laboratories, Nippon Telegraph and Telephone Corporation, Atsugi 243-0198, Japan (e-mail: daisuke.niizumi@ntt.com; d.takeuchi@ntt.com; yasunori.ohishi@ntt.com; harada.noboru@ntt.com; kunio.kashino@ntt.com)

Considering realistic applications, the scope of this study extends to the pre-training of representations specialized for application tasks. Conventional methods evaluate a general-purpose audio representation pre-trained on a large dataset with benchmarks of various tasks [19]–[21]. While a general-purpose representation is usually fine-tuned to solve the application tasks, the performance can be insufficient if the data distribution of the task differs from that of the pre-training. For example, private and confidential data are often used in the industrial and medical fields, and we cannot expect the data distribution of such data to be close to that of a public pre-training dataset. On the other hand, previous studies [22], [23] showed that training on the task data or on data from the same domain is effective, and we consider such training a practical solution.

Therefore, we propose M2D for X (M2D-X), an extension of M2D, to learn specialized representations of application tasks [Fig. 1(b)]. The application task may require learning from information such as labels and domain techniques to gain sufficient performance. In addition, the application data may be small, as in the industrial and medical domains, making learning by masked prediction challenging [24], [25]. M2D-X is a multitask learning framework that adds an additional domain-specific learning task and a denoising task using background noise to M2D. To accommodate various application demands, we leave freedom with the choice of additional learning tasks, such as supervised learning of application labels, distillation of domain models, or regularizing M2D from overfitting. Background noise helps in learning from small data with data augmentation effects and forms a denoising task that makes the representation robust. As a result, M2D-X should serve as a universal audio pre-training framework that addresses the diverse needs of audio applications.

Experiments with three settings—general audio with large-scale datasets, competitive speech representation, and medical applications with small data—confirmed that M2D and M2D-X achieve top-level performance, demonstrating their potential to serve various applications as a pre-training framework. We find that encoding only the masked parts of the input to obtain a training signal improves masked prediction-based SSL, that combining supervised learning with M2D SSL enhances specialized performance on top of the general-purpose performance, and that M2D-X configured for regularization using background noise enables successful further pre-training on small data. Our contributions include:

- We propose a new masked prediction-based SSL, M2D, and show that it learns general-purpose audio representations with top-level performance.
- We propose M2D-X that extends M2D and succeeds in learning representations specialized to applications with top-level performance. To our knowledge, this is the first study to conduct pre-training on application data in addition to general-purpose data in the audio domain.
- We provide a realistic example of small data under a restricted data/computational resource setting with our code and the pre-trained weights for future studies<sup>1</sup>.

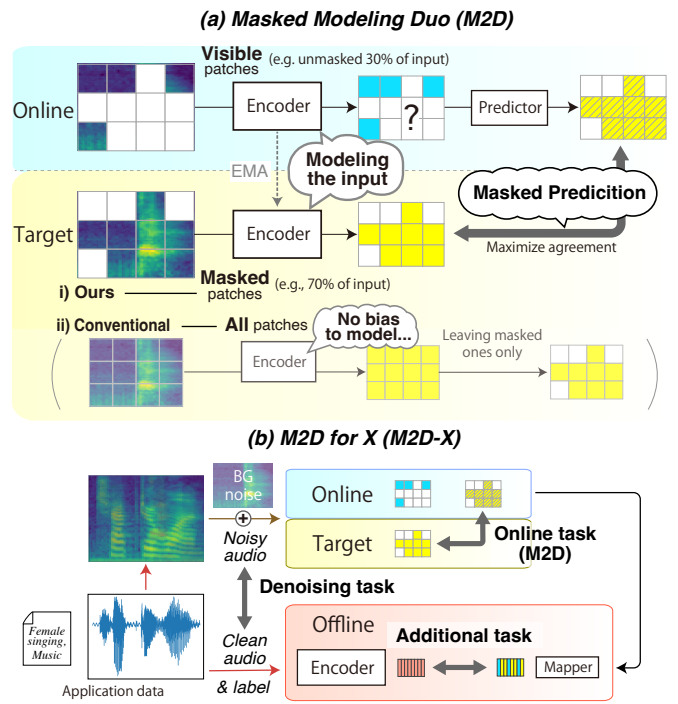


Fig. 1. (a) M2D overview. The online network encodes the visible patches of the randomly masked input signal, while the target network encodes the masked patches. M2D encourages both representations to model the input signal through a task to predict the target representation using the online representation. (b) M2D-X overview. Introducing background noise and offline network allows M2D-X to learn from M2D, denoising, and an additional task, enabling pre-training of specialized representations for diverse applications.

## II. RELATED WORK

### A. Relationship with our previous work

We introduced M2D [26] and M2D for Speech (M2D-S) [27] in our previous work for learning general-purpose audio and speech representations. This paper redefines the M2D family and explores its potential as an application-agnostic audio pre-training framework.

We refine M2D and introduce positional encoding interpolation (Section III-A2) to handle variable-length audio in fine-tuning. We also improve and stabilize the experiments by using the statistics of the pre-training dataset (e.g., AudioSet [28]) for standardizing spectrograms instead of that of downstream tasks, and by introducing fine-tuning parameters SpecAugment [29], Adjust positional encoding, and Freeze embedding layer as listed in Table II (Section IV-B). We extend M2D-S to an application-agnostic framework and redefine it as M2D for X (M2D-X) (Section III-B). M2D-X redesigns the M2D-S offline network, making it possible to configure an additional learning task to meet various application needs.

### B. Background: Image SSL

Our M2D was inspired by MAE [3] for an effective masked prediction-based SSL and Bootstrap Your Own Latent [30] (BYOL) as a framework for directly learning latent representations using a target network. MAE learns to reconstruct the input data, whereas our M2D learns to predict masked latents, and BYOL does not learn the masked prediction task.

SIM [4], MSN [5], and data2vec [18] learn to predict masked patch representations using a target network, but,

<sup>1</sup><https://github.com/nttcs-lab/m2d>

unlike ours, the target network inputs all patches. CAE [6] and SplitMask [7] encode target representations using only masked patches like ours does, but without the use of a target network. All methods above learn image representations, and data2vec also learns speech and audio representations.

### C. Speech and Audio SSL using Transformer

SSL methods that train transformers with masked prediction have shown promising performance in various domains. Speech representation models, such as Mockingjay [31] and TERA [32], take spectrograms as input. Similar to general-purpose models, TERA employs a masking strategy for splitting both frequency bins and time steps. SOTA models, such as wav2vec2.0 [8], BigSSL [33], data2vec [18], HuBERT [9], and WavLM [11], take speech waveforms as input to learn representations. Notably, models such as wav2vec2.0, HuBERT, and WavLM effectively learn by using discretized pseudo-labels with vector quantization or clustering of pre-trained model features. Methods similar to our M2D-X include MT4SSL [34] and M-CTRL [35] for network configuration, DistillHuBERT [36] for distillation, WavLM and Wang et al. [37] for denoising, and RobustDistiller [38] for distillation and denoising; these methods learn speech representations.

General-purpose representation models, such as SSAST [12], ATST [39], MAE-AST [14], MaskSpec [15], MSM-MAE [16], Audio-MAE [13], and BEATs [21], have shown SOTA performance. They typically take spectrograms as acoustic feature input, split input on both the time and frequency axes, and train a Vision Transformer (ViT) [17], but differ from ours in that they do not learn from predicting the representations encoded on masked patches only. Other audio SSL methods using non-ViT encoders, e.g., BYOL-A [20], Wang et al. [40], and DeLoRes [41] do not learn from masked prediction.

### D. Learning Specialized Representations

In previous work similar to that described in this paper, Melms et al. [42] and BYOL-S [43] have specialized a general-purpose model BYOL-A [20] in medical and speech applications. SSAST has adapted the patch size and pre-training dataset and compared results with speech models on SUPERB. In the NLP domain, LIBERT [44] specializes BERT [1] using an additional task for pre-training a lexically informed BERT, a multitask learning setting similar to ours.

Further pre-training using data from the target task or its domain has been studied in the NLP domain; note that it is different from continuous learning, where a model learns a new task without forgetting the previously learned tasks. Sun et al. [45] reported that further pre-training using data from the task domain is effective when the target task data is small. In contrast, Zhu et al. [46] reported that further pre-training using data from the task domain is not always effective when the target task data is sufficient. In the image domain, Lee et al. [47] use MAE for further pre-training, and their configuration of combining distillation to avoid overfitting is similar to our M2D-X. Meanwhile, we introduce the use of background noise and a denoising task for further pre-training of sound.

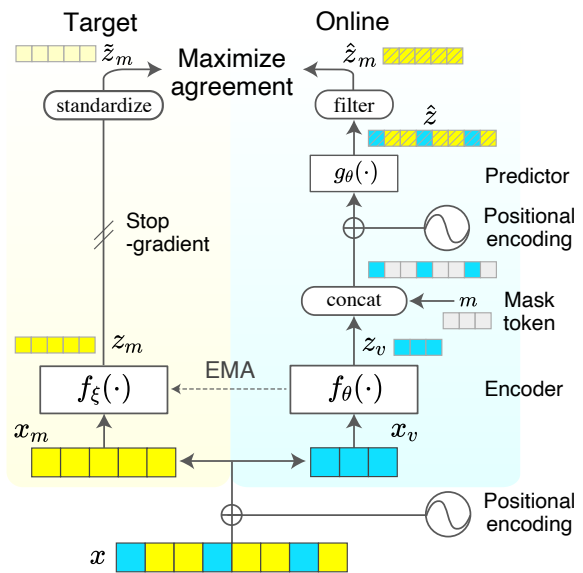


Fig. 2. M2D pre-training flow. The online network encodes the visible patch  $x_v$  and predicts the representation  $\tilde{z}_m$  of the masked patch  $x_m$  encoded in the target network. M2D learns the representation by maximizing the agreement between the prediction  $\hat{z}_m$  and  $\tilde{z}_m$ .

## III. PROPOSED METHODS

We propose Masked Modeling Duo (M2D), an improved masked prediction SSL, and M2D for X (M2D-X), a method for learning representations specialized for an application  $X$ .

### A. Masked Modeling Duo

M2D is an SSL method that learns by predicting the representation of masked patches from the representation of unmasked (visible) patches. As shown in Fig. 2, M2D consists of online and target networks. The online network encodes the visible patches into a representation and predicts the masked patch representation. Meanwhile, the target network does not use the information from the visible patches but encodes only the masked patches into the representation as training signals. While conventional methods give all patches to the target network, the information we provide to each network is exclusive.

1) *Pre-training*: M2D first splits the input into masked and visible patches, processes them in two networks, calculates the loss, and finally updates the entire network.

**Processing input.** The framework partitions the input data  $x$  (audio spectrogram, image, etc.) into a grid of patches, maps them with a learnable linear layer (patch embedding layer), adds positional encoding, and randomly selects a number of patches according to a masking ratio as masked patches  $x_m$  (e.g., 70% of the input) and the rest as visible patches  $x_v$  (e.g., the remaining 30%). While we use the same positional encoding as MAE [3], we tested various masking ratios as discussed in Section IV-B3.

**Online and target networks.** The online network, defined by a set of weights  $\theta$ , uses the online encoder  $f_\theta$  to encode the visible patches  $x_v$  into the representation  $z_v = f_\theta(x_v)$ . It concatenates shared, learnable masked tokens  $m$  to  $z_v$ , adds

the positional encoding  $p$ , and predicts  $\hat{z}$ , representations of all input patches, using the predictor  $g_\theta$ .

$$\hat{z} = g_\theta(\text{concat}(z_v, m) + p) \quad (1)$$

It then filters the prediction result  $\hat{z}$  to output  $\hat{z}_m = \{\hat{z}[i] \mid i \in I_M\}$  containing only masked patch representations, where  $I_M$  is the set of indices of the masked patches.

The target network is defined by parameter  $\xi$  and consists only of momentum encoder  $f_\xi$ , which is identical to the online encoder except for the parameter. The network encodes masked patches  $x_m$  using  $f_\xi$  to output the representation  $z_m = f_\xi(x_m)$ . We then standardize  $z_m$  to  $\tilde{z}_m = (z_m - \text{mean}(z_m)) / \sqrt{\text{var}(z_m)}$ . We do this to stabilize the training, which we empirically confirmed in preliminary experiments, rather than for performance gain as in MAE.

**Loss function.** The loss is calculated using the standardized target output  $\tilde{z}_m$  as a training signal against the online prediction output  $\hat{z}_m$ . Inspired by BYOL [30], we calculate the loss  $L_{m2d}$  by the mean square error (MSE) of  $l_2$ -normalized  $\hat{z}_m$  and  $\tilde{z}_m$ .

$$L_{m2d} = \|l_2(\hat{z}_m) - l_2(\tilde{z}_m)\|_2^2 = 2 - 2 \cdot \frac{\langle \hat{z}_m, \tilde{z}_m \rangle}{\|\hat{z}_m\|_2 \cdot \|\tilde{z}_m\|_2}, \quad (2)$$

where  $\langle \cdot, \cdot \rangle$  denotes the inner product.

**Updating network parameters.** Our framework updates parameters  $\theta$  and  $\xi$  after each training step. It updates  $\theta$  only by minimizing the loss  $L_{m2d}$  as depicted by the stop-gradient in Fig. 2, whereas updating  $\xi$  is based on a slowly moving exponential average of  $\theta$  with a decay rate  $\tau$ :

$$\xi \leftarrow \tau \xi + (1 - \tau) \theta \quad (3)$$

It has been empirically shown that stop-gradient operation helps avoid collapsing to an uninformative solution and that the moving-average behavior may lead to learning effective representations [30], [48]. After the training, we transfer only the  $f_\theta$  as a pre-trained model.

2) *Transferring Models to Audio Tasks:* While the model's input duration is fixed, we provide two ways to encode variable-length audio into features so that we can transfer the pre-trained models to tasks with any audio length. In addition, we convert the model's per-patch output features into a sequence of time-framed feature vectors.

**Encoding variable-length audio.** The first way splits the input audio data by the model's input duration, encodes each separately, and then concatenates them. The second is a common practice, where we interpolate the model's positional encoding to match the audio length of the task so that the model can encode long audio at once. The former method can exploit the learned knowledge even when the model is frozen, while the latter can transfer the learned knowledge by fine-tuning it to the interpolated positions. We applied the former in most cases and the latter only when fine-tuning with an audio length close to that of pre-training.

**Converting feature into a sequence.** We adopt the MSM-MAE [16] feature calculation to enable the processing of

features on a time-frame basis. The pseudo-code for the calculation follows:

$$\begin{aligned} z' &= z.\text{reshape}(B, N_F, N_T, D) \\ &.\text{transpose}(1, 2) \\ &.\text{reshape}(B, N_T, N_F D), \end{aligned} \quad (4)$$

where  $z \in R^{B \times N_F \times N_T \times D}$  is the encoder output,  $B$  is batch size,  $N_F$  is the number of patches along frequency,  $N_T$  is the number of patches along time,  $D$  is a feature dimension, and  $z' \in R^{B \times N_T \times N_F D}$  is the calculation result.

This calculation makes it easier to subsequently compute statistics along time frames, e.g., temporal average pooling. We summarize an audio clip-level feature  $z'' = 1/N_T \sum_{t=1}^{N_T} z'[t]$ , averaging  $z'$  over time in the experiments. For example,  $z''$  becomes a 3840-d feature, where  $D = 768$  and  $N_F = 5$ .

## B. Masked Modeling Duo for X

M2D-X is a pre-training framework designed to learn a representation specialized to the data distribution of an application  $X$ , even with small data. As shown in Fig. 3, it extends M2D with an offline network and adds background noise input. The additional task in the offline network is configurable to accommodate the various application needs. To form a denoising task, the offline network inputs clean application data (audio and labels), while M2D inputs noisy audio mixed with application audio and background noise.

We incorporate background noise to enable successful pre-training on the application data. Background noise creates the effect of data augmentation, which is especially helpful for small datasets, and the denoising task, which contributes to learning a robust representation focused on the application data distribution.

1) *Offline Network:* As illustrated in Fig. 3(b), the offline network computes the loss from the audio features encoded in M2D and the training signal obtained from the application data. The  $z_v$  and  $\hat{z}_m$  from the M2D branch are concatenated and reshaped using (4) to obtain the audio feature  $\hat{h}$  per time frame. The offline encoder converts the application data  $y_{\text{audio}}$  and/or  $y_{\text{label}}$  into the training signal  $\tilde{y}$ . The offline loss  $L_{\text{off}}$  is calculated using  $\tilde{y}$  and  $\hat{h}'$  converted from  $\hat{h}$  by the online mapper. The actual loss function depends on the application scenario, e.g., MSE loss in (2) or cross-entropy loss.

This branch network naturally forms a denoising task by calculating the loss between the noisy audio M2D features and the clean application data (audio/labels). As a result, the entire network learns from a multi-task of M2D, an additional task using the offline loss, and a denoising task.

2) *Noisy Audio:* The noisy audio  $x_{\text{noisy}}$  is obtained by mixing the target log-mel spectrogram data  $x_{\text{targ}}$  and background log-mel spectrogram data  $x_{\text{bg}}$  with the dataset noise ratio  $\eta$ . This process is expressed by the following equation as in [49].

$$x_{\text{noisy}} = \log((1 - \eta) \exp(x_{\text{targ}}) + \eta \exp(x_{\text{bg}})) \quad (5)$$

Although pre-training with masked prediction requires a large dataset [24], [25], mixing large datasets such as AudioSet

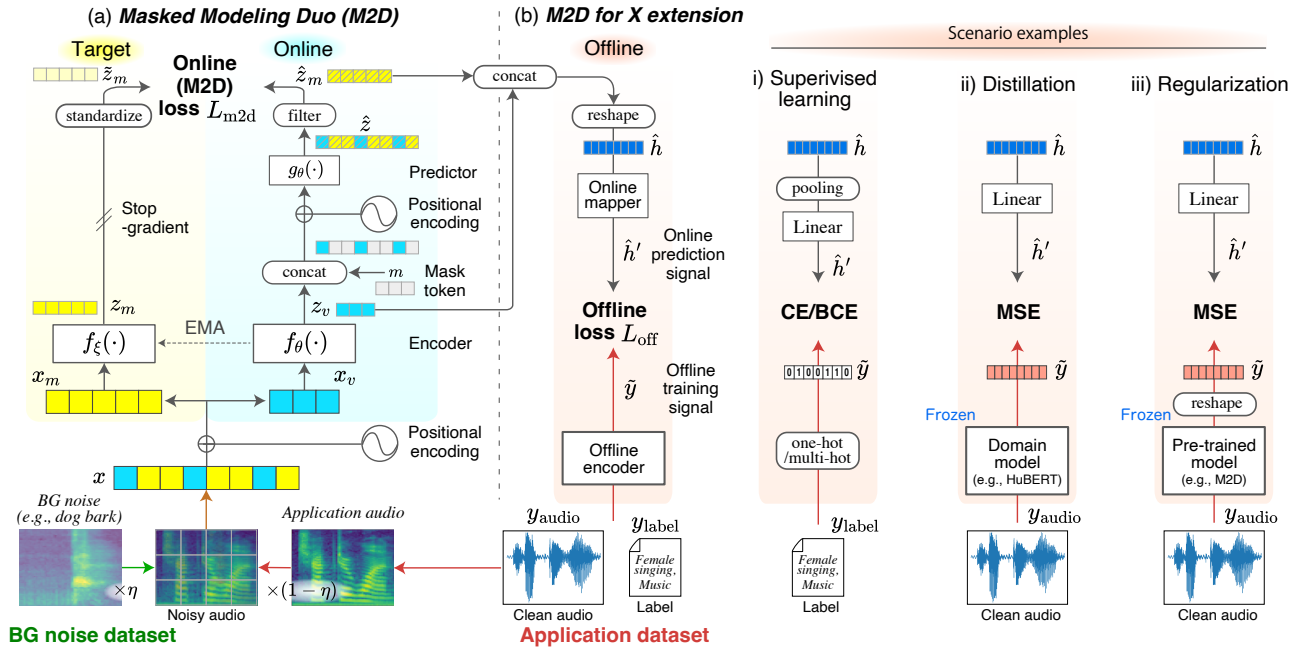


Fig. 3. M2D-X pre-training flow and application scenarios. M2D-X adds an offline network to M2D and inputs background noise, forming a multitask of M2D, a denoising task, and an additional task. Scenario examples show the offline network configurations to compose an additional task for each purpose: supervised learning of task labels, distilling a domain pre-trained model, or regularizing to prevent overfitting M2D to a small dataset.

leads to the effect of data augmentation, allowing the pre-training of effective representations even with a small target dataset.

3) *M2D-X Pre-training*: In the M2D-X framework, M2D performs its training process described in Section III-A1 and calculates loss  $L_{m2d}$ , while the offline network calculates its loss,  $L_{off}$ . The overall M2D-X loss  $L_{m2dX}$  is then calculated by combining  $L_{m2d}$  and  $L_{off}$ :

$$L_{m2dX} = \lambda_{m2d} L_{m2d} + \lambda_{off} L_{off}, \quad (6)$$

where the loss weights  $\lambda_{m2d}$  and  $\lambda_{off}$  control the contribution. M2D-X updates the weights of the entire network by back-propagating  $L_{m2dX}$ .

4) *Specialized Learning Scenarios*: As shown in the scenario examples in Fig. 3(b), the M2D-X framework enables pre-training specialized to the application by adopting an online mapper, an offline encoder, and an offline loss function for each application.

**i) Supervised Learning.** This scenario pre-trains a suitable representation for the application’s training signal. The online mapper combines temporal pooling (e.g., average pooling) and a linear layer to convert  $\hat{h}$  into  $\hat{h}'$ . The offline network forms a task of conventional supervised learning by calculating the cross-entropy (CE) or binary cross-entropy (BCE) loss between one-hot or multi-hot encoded labels. These loss functions should help build a distribution of the audio representation suitable for representing the application’s class definition. Section IV-C evaluates this scenario.

**ii) Distillation.** This scenario distills the learned knowledge when a domain-specific model already exists. The domain model features can be distilled by using a linear layer for the online mapper, a frozen domain pre-trained model for

the offline encoder, and MSE loss, for example. Section IV-D evaluates this scenario.

**iii) Regularization.** Problems typically found in confidential and proprietary data in domains such as industrial and medical domains are a small dataset and a data distribution different from that of a general large pre-training dataset. In the regularization scenario, we address these problems by using an enhanced further pre-training strategy based on distillation. Further pre-training is a strategy where a pre-trained model is pre-trained on a target dataset [47] to make the model effective for the target while utilizing the learned knowledge in the previous pre-training.

We use the original pre-trained model as a frozen offline encoder and its weights to initialize M2D online encoder weights, forming a distillation, the same as in the previous scenario. Then, the offline encoder with frozen weights maintains its features to follow the original pre-training data distribution even with the target data input and helps prevent the M2D online encoder from overfitting on a small dataset while further pre-training. Section IV-E evaluates this scenario.

The first two scenarios enhance conventional supervised learning and distillation combined with effective masked prediction-based learning of M2D, while the regularization scenario enhances further pre-training. As described in these examples, our aim is for M2D-X to serve as a universal audio pre-training framework for diverse applications.

## IV. EXPERIMENTS

In the experiments, we evaluated learning of a general-purpose audio representation with M2D, followed by learning of specialized representations with M2D and M2D-X. Experiments included three audio settings: general audio, speech, and a medical application sound. In a scenario of general

TABLE I  
EVALUATION IV-B GENERAL-PURPOSE AUDIO REPRESENTATION: DOWNSTREAM TASK DETAILS.

	Environmental sound tasks				Speech tasks				Music tasks		
	AS2M [28]	AS20K [28]	ESC-50 [50]	US8K [51]	SPCV2 [52]	VC1 [53]	VF [53]	CRM-D [54]	GTZAN [55]	NSynth [56]	Surge [57]
Evaluation protocol <sup>†</sup>	FT	FT	FT / LE	LE	FT / LE	FT / LE	LE	LE	LE	LE	LE
No. of training samples	2,005,132	21,940			84,843	138,361	121,281	5155	443	289,205	148,896
No. of validation samples	-	-	5 folds	10 folds	9981	6904	26,684	732	197	12,678	17,160
No. of test samples	20,178	20,178	2000	8732	11,005	8251	28,463	1551	290	4096	17,336
No. of classes	527	527	50	10	35	1251	6	6	10	11	88
Average duration	10.0 s	10.0 s	5.0 s	4.0 s	1.0 s	8.2 s	5.8 s	2.5 s	30.0 s	4.0 s	4.0 s

<sup>†</sup> FT and LE stand for fine-tuning and linear evaluation, respectively.

TABLE II  
EVALUATION IV-B GENERAL-PURPOSE AUDIO REPRESENTATION:  
FINE-TUNING SETTINGS

Parameter	AS2M	AS20K	ESC-50	SPCV2	VC1
Learning rate	2.0	0.5	0.5	0.5	0.0005
Batch size	64	64	128	128	64
Optimizer	LARS	SGD	SGD	SGD	AdamW
Mixup ratio	0.5	0.3	0.0	0.3	0.0
Random resize crop	-	✓	✓	✓	-
SpecAugment <sup>‡</sup> [29]	30/192	30/192	15/48	30/48	30/48
Training epochs (total)	70	200	200	200	50
Training epochs (warm-up)	15	5	5	5	5
Structured Patchout [58] ratio	0.5	0.5	0.5	0.5	0.0
Adjust positional encoding	✓	✓	-	-	✓
Freeze embedding layer [59]	-	-	✓	-	-

<sup>‡</sup> The frequency/time masking parameters.

audio with a large-scale dataset, M2D learns a general-purpose audio representation (Section IV-B), and M2D-X learns a specialized representation of AudioSet (Section IV-C). To assess the performance in a highly competitive domain, M2D and M2D-X learn specialized speech representations (Section IV-D). To assess applicability to a small-data regime, M2D and M2D-X learn specialized representations for medical applications (Section IV-E) under a further pre-training strategy. Through these experiments, we validated the effectiveness of our methods as a universal audio pre-training framework.

### A. Basic Experimental Setup

We conducted experiments using the following basic implementations and settings. To facilitate comparison with previous studies, we implemented M2D based on the MAE implementation with minimal modifications; specifically, we implemented an additional target network on top of the MAE code, adopted the MAE decoder as our predictor  $g_\theta$  without changes, and used vanilla ViT-Base [17] with a 768-d output feature as our encoders ( $f_\theta$  and  $f_\xi$ ) for all experiments. Our basic settings are: input audio length of 6 s, the same as in ATST [39]; patch size of  $16 \times 16$ , the same as in most studies [12]–[15]; and the masking ratio of 0.6 and 0.7, which performed well in preliminary experiments.

While we used ViT as is for the encoder, we implemented the feature calculation optimized for audio, as described in Section III-A2. In the fine-tuning evaluation, the weights of the patch embedding layer were fixed in order to stabilize the fine-tuning [59] for some tasks.

We preprocessed audio samples to a log-scaled mel spectrogram with a sampling frequency of 16,000 Hz, window size of 25 ms, hop size of 10 ms, and mel-spaced frequency bins  $F = 80$  in the range of 50 to 8000 Hz. We standardized spectrograms with the statistics of the pre-training dataset (e.g., average  $-7.1$  and standard deviation  $4.2$  for AudioSet). The

input spectrogram with the default input duration of 6 s has a size of  $80 \times 608$  (Freq. bins  $\times$  Time frames), making  $N_F = 5$  and  $N_T = 38$  with patch size of  $16 \times 16$ .

For pre-training, we set the number of epochs as 300, the number of warm-up epochs as 20, batch size as 2048, and the base learning rate as  $3e-4$ . All other settings were the same as in the MAE, including the learning rate scheduling and optimizer. The EMA decay rate  $\tau$  for the target network update was linearly interpolated from 0.99995 at the start of training to 0.99999 at the end. Appendix B describes the required computational resources.

For linear evaluation and fine-tuning, we used typical random seeds (e.g., 42), ran each evaluation six times, and averaged the results with 95% confidence intervals.

### B. Evaluation: General-purpose Audio Representation

In this experiment, we validated that M2D learns a general-purpose audio representation that performs well. We pre-trained M2D on a large-scale general audio dataset, AudioSet, and evaluated it in linear evaluation and fine-tuning.

We pre-trained models with the basic setup described in Section IV-A on AudioSet [28] with 2,005,132 samples (5569 h) of 10-s audio from the balanced and unbalanced train segments. We randomly cropped 6-s audio from a 10-s sample. Table I lists the downstream tasks used in the evaluation. These are various sound classification tasks, and results are accuracies or mean average precision (mAP). When a task’s dataset contained variable-length audio, we randomly cropped or zero-padded the average audio length for each sample to create a batch of length-aligned audio fed into the model.

- AudioSet [28]: a multi-label audio event classification task with two settings. AS2M uses all 2M training samples, whereas AS20K uses 21K samples from the balanced train segments for training.
- ESC-50 [50]: an environmental sound classification task with 50 classes. We follow standard leave-one-out cross-validation (LOOCV) with the official five folds.
- UrbanSound8K [51] (US8K): an urban sound classification task. We follow the official ten-fold LOOCV.
- Speech Commands V2 [52] (SPCV2): a speech command word classification task.
- VoxCeleb1 [53] (VC1): a speaker identification task with interviews of 1251 celebrities.
- VoxForge [60] (VF): a language identification task.
- CREMA-D [54] (CRM-D): a speech emotion recognition task for 91 speakers. We follow [20] for the data splits.
- GTZAN [55]: a music genre recognition task. We follow fault-filtered partitioning [61] [62].

TABLE III  
EVALUATION IV-B GENERAL-PURPOSE AUDIO REPRESENTATION: LINEAR EVALUATION RESULTS (%) WITH 95% CI.

Model (/masking ratio)	# Params	Env. sound tasks		Speech tasks				Music tasks			Avg.
		ESC-50	US8K	SPCV2	VC1	VF	CRM-D	GTZAN	NSynth	Surge	
<i>(Previous SSL methods)</i>											
DeLoRes-M [41]	5.3M	-	82.7	89.7	45.3	88.0	-	-	75.0	-	-
SF NFNNet-F0 [40]	63M	91.1	-	93.0	64.9	90.4	-	-	<b>78.2</b>	-	-
BYOL-A [20]	5.3M	83.2 ± 0.6	79.7 ± 0.5	93.1 ± 0.4	57.6 ± 0.2	93.3 ± 0.3	63.8 ± 1.0	70.1 ± 3.6	73.1 ± 0.8	37.6 ± 0.3	72.4
ATST Base [39]†	86M	<b>94.1 ± 0.6</b>	85.8	95.1	72.0	97.6 ± 0.0	68.8 ± 1.3	78.9 ± 3.5	76.2	32.8 ± 0.0	77.9
BEAT <sub>Siter3</sub> [21]†	90M	86.9 ± 1.4	84.8 ± 0.1	89.4 ± 0.1	41.4 ± 0.7	94.1 ± 0.3	64.7 ± 0.8	72.6 ± 4.3	75.9 ± 0.2	39.3 ± 0.4	72.1
<i>(i) Baseline: MAE variant</i>											
MSM-MAE/0.75 [16]	86M	89.2 ± 0.9	87.4 ± 0.2	96.0 ± 0.1	73.6 ± 0.2	97.8 ± 0.2	71.2 ± 0.4	79.2 ± 0.9	74.6 ± 0.9	<b>43.3 ± 0.3</b>	79.1
<i>(ii) Conventional: M2D variants that feed all patches to the target network</i>											
M2D/0.6 (all patches→target)	86M	90.5 ± 0.4	87.0 ± 0.3	96.0 ± 0.1	<b>76.1 ± 0.2</b>	97.8 ± 0.1	72.7 ± 0.8	81.3 ± 2.7	75.2 ± 0.1	41.2 ± 0.2	79.7
M2D/0.7 (all patches→target)	86M	91.0 ± 0.2	86.7 ± 0.3	96.2 ± 0.1	72.5 ± 0.2	98.2 ± 0.0	72.5 ± 1.1	<b>85.2 ± 2.4</b>	76.8 ± 0.2	41.9 ± 0.2	80.1
<i>(iii) Ours</i>											
M2D/0.6	86M	91.6 ± 0.5	87.2 ± 0.3	<b>96.2 ± 0.1</b>	75.0 ± 0.3	98.2 ± 0.1	71.4 ± 0.9	83.4 ± 3.6	76.1 ± 0.1	41.7 ± 0.2	80.1
M2D/0.7	86M	91.3 ± 0.6	<b>87.6 ± 0.2</b>	96.0 ± 0.1	73.4 ± 0.2	<b>98.3 ± 0.0</b>	<b>73.0 ± 0.7</b>	84.1 ± 2.7	75.7 ± 0.1	42.1 ± 0.2	<b>80.2</b>
<i>(Reference supervised learning methods and SSL with )</i>											
AST [19]†	86M	93.5 ± 0.4	85.5 ± 0.2	71.8 ± 0.4	16.5 ± 0.4	81.2 ± 0.2	57.9 ± 0.6	84.3 ± 1.8	73.2 ± 0.2	25.8 ± 0.2	65.5
AST-Fusion#5#12 [65]	86M	94.2	85.5	80.4	24.9	87.6	60.7	82.9	77.6	34.6	69.8
HTS-AT [66]†	31M	<b>95.7 ± 0.7</b>	83.8 ± 0.1	82.1 ± 0.3	18.1 ± 0.4	82.3 ± 0.3	56.2 ± 0.6	85.1 ± 0.5	73.3 ± 0.8	26.3 ± 0.5	67.0
BEAT <sub>Siter3+</sub> [21]†	90M	95.5 ± 0.3	87.6 ± 0.3	86.7 ± 0.1	37.0 ± 0.2	92.5 ± 0.1	67.6 ± 1.5	84.6 ± 0.5	73.1 ± 0.4	35.7 ± 0.3	73.4

† The results with CI value were obtained in [20], [26], and this study using publicly available pre-trained models.

- NSynth [56]: an instrument family classification task.
- Pitch Audio Dataset (Surge synthesizer) [57] (Surge): a pitch audio classification task composed of 88 MIDI note classes. We follow [20] for the data splits.

We followed BYOL-A [20] to use a unified evaluation platform, EVAR<sup>2</sup>, for linear evaluation and fine-tuning. We used the MSM-MAE [16], an MAE variant for audio, as a baseline MAE for comparison. We transferred the pre-trained MSM-MAE in the same way as with M2D described in Section III-A2 for fair comparison while keeping pre-training parameters the same as in the original MAE, such as the masking ratio of 0.75. Preliminary experiments verified that the MSM-MAE outperforms a vanilla MAE.

**Linear evaluation details.** We followed BYOL-A [20] for the linear evaluation procedure. The evaluation pipeline first converts downstream task samples into features using a *frozen* pre-trained model, trains a linear layer with task labels, and then conducts tests to get the results. We used the validation set for early stopping with a patience of 20 epochs and trained the linear layer for up to 200 epochs using the Adam optimizer and a learning rate of 0.00003.

**Fine-tuning details.** We used the tasks commonly used in previous studies, namely ESC-50, SPCV2, and VC1, the same as in the linear evaluation, plus AS20K and AS2M. The fine-tuning pipeline follows ATST [39] and Audio-MAE [13]. A linear classifier was added on top of the pre-trained model to train the entire network. We used SpecAugment [29], Mixup [20], [63], and Random Resize Crop (RRC) [20] for data augmentation, along with Structured Patchout proposed in PaSST [58] that masks patches during training. We used SGD, LARS, and AdamW for the optimizer and Cosine annealing [64] for learning rate scheduling. For AS-2M, we used a weighted sampler as in Audio-MAE, sampling 200K data without replacement for each epoch. We used the hyperparameters for each task as listed in Table II. When using the Structured Patchout, we used 768-d features calculated by averaging all ViT outputs because (4) is not applicable to the masked patches.

<sup>2</sup><https://github.com/nttcs/eval-audio-repr>

TABLE IV  
EVALUATION IV-B GENERAL-PURPOSE AUDIO REPRESENTATION: FINE-TUNING RESULTS WITH 95% CI.

Model (/masking ratio), # Params	AS2M mAP	AS20K mAP	ESC-50 acc(%)	SPCV2 acc(%)	VC1 acc(%)
<i>(Previous SSL methods)</i>					
DeLoRes-M [41], 5.3M	-	-	-	96.0	62.0
MAE-AST [14], 86M	-	30.6	90.0	98.0	63.3
MaskSpec /-small [15], 86M	47.1	32.3	90.7	97.7	-
SSAST 250/400/Frame [12], 89M	-	31.0	88.8	98.2	80.8
data2vec [18], 94M	-	34.5	-	-	-
Audio-MAE (local) [13], 86M	47.3	37.1	94.1	98.3	94.8
ATST Base [39], 86M	-	37.4	-	98.0	94.3
BEAT <sub>Siter3</sub> [21], 90M	<b>48.0</b>	38.3	95.6	98.3	-
<i>(i) Baseline: MAE variant</i>					
MSM-MAE/0.75 [16], 86M	47.4 ± 0.1	37.9 ± 0.0	95.4 ± 0.1	98.4 ± 0.0	96.6 ± 0.1
<i>(ii) Conventional: M2D variants that feed all patches to the target network</i>					
M2D/0.6 (all patches→target), 86M	47.4 ± 0.2	37.6 ± 0.1	95.4 ± 0.3	98.4 ± 0.0	<b>96.6 ± 0.3</b>
M2D/0.7 (all patches→target), 86M	47.6 ± 0.0	38.3 ± 0.0	95.8 ± 0.2	98.4 ± 0.0	96.0 ± 0.1
<i>(iii) Ours</i>					
M2D/0.6, 86M	47.7 ± 0.2	38.4 ± 0.1	95.6 ± 0.1	<b>98.5 ± 0.1</b>	96.5 ± 0.1
M2D/0.7, 86M	47.9 ± 0.0	<b>38.6 ± 0.1</b>	<b>96.0 ± 0.2</b>	98.4 ± 0.1	96.3 ± 0.2
<i>(Reference supervised learning method results)</i>					
AST (Single)-PS [19], 86M	45.9	34.7	95.6	98.11	-
EAT-S/M [67], 25.5M	42.6	-	96.3	98.15	-
PaSST [58], 86M	47.1	-	96.8	-	-
HTS-AT [66], 31M	47.1	-	97.0	98.0	-
BEAT <sub>Siter3+</sub> [21], 90M	<b>48.6</b>	<b>41.8</b>	<b>98.1</b>	98.1	-

1) *Comparison with Baselines:* We compare the results for (i) MAE on which our methods are based, (ii) the conventional method that gives all patches to the target network, and (iii) our M2D in Tables III and IV. We used the same codebase to obtain these results; only the learning algorithm differed.

Table III shows linear evaluation results. Compared to (i) MAE, (iii) M2D outperforms MAE with about a +1.0 average performance improvement on most tasks, demonstrating the effectiveness of predicting the representation instead of reconstructing the input signal during pre-training. On the other hand, MAE outperforms ours on the pitch classification task Surge, suggesting that MAE extracts more frequency-related information. The average performance improvement of (iii) M2D over (ii) Conventional is +0.4 at masking ratios of 0.6 and +0.1 at 0.7, which is small, but indicates an overall performance improvement, supporting the effectiveness of the proposed method to feed only masked patches instead of providing all input signals to the target network.

Table IV shows fine-tuning results. (iii) M2D performed better than (i) MAE and (ii) Conventional on most tasks, while underperforming others on VC1, which requires detailed information to differentiate the 1251 speakers. We think the

TABLE V  
EVALUATION IV-C SPECIALIZED REPRESENTATION FOR AUDIOSET: LINEAR EVALUATION RESULTS (%) WITH 95% CI.

Model (/masking ratio)	# Params	Env. sound tasks			Speech tasks			Music tasks			Avg.
		ESC-50	US8K	SPCV2	VC1	VF	CRM-D	GTZAN	NSynth	Surge	
AST [19] <sup>†</sup>	86M	93.5 ± 0.4	85.5 ± 0.2	71.8 ± 0.4	16.5 ± 0.4	81.2 ± 0.2	57.9 ± 0.6	84.3 ± 1.8	73.2 ± 0.2	25.8 ± 0.2	65.5
HTS-AT [66] <sup>†</sup>	31M	95.7 ± 0.7	83.8 ± 0.1	82.1 ± 0.3	18.1 ± 0.4	82.3 ± 0.3	56.2 ± 0.6	85.1 ± 0.5	73.3 ± 0.8	26.3 ± 0.5	67.0
BEAT <sub>Siter3+</sub> [21] <sup>†</sup>	90M	95.5 ± 0.3	87.6 ± 0.3	86.7 ± 0.1	37.0 ± 0.2	92.5 ± 0.1	67.6 ± 1.5	84.6 ± 0.5	73.1 ± 0.4	35.7 ± 0.3	73.4
M2D-AS/0.7	86M	<b>96.1 ± 0.6</b>	<b>89.8 ± 0.2</b>	95.7 ± 0.0	68.3 ± 0.4	<b>98.4 ± 0.0</b>	<b>73.1 ± 0.6</b>	<b>86.9 ± 0.6</b>	75.2 ± 0.2	41.7 ± 0.3	<b>80.6</b>
<i>(Reference: The M2D model pre-trained in Section IV-B)</i>											
M2D/0.7	86M	91.3 ± 0.6	87.6 ± 0.2	<b>96.0 ± 0.1</b>	<b>73.4 ± 0.2</b>	98.3 ± 0.0	73.0 ± 0.7	84.1 ± 2.7	75.7 ± 0.1	<b>42.1 ± 0.2</b>	80.2

<sup>†</sup> The results were obtained in [20], [26], and this study using publicly available pre-trained models.

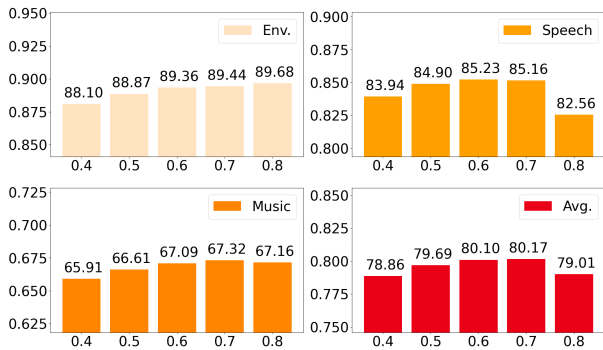


Fig. 4. Evaluation IV-B General-purpose audio representation: Masking ratio ablation average linear evaluation results (%).

reason is similar to that for the performance drop on Surge in Table III; M2D may have learned to model more abstract information than the details. Overall, these results support the effectiveness of M2D.

2) *Comparison with SOTA Models:* M2D achieves the best results on four out of nine tasks in linear evaluation (Table III) and three out of five in fine-tuning (Table IV), confirming its effectiveness in learning general-purpose audio representations. While achieving good performance on average, M2D underperforms with ATST on ESC-50 in linear evaluation and BEATs on AS2M in fine-tuning. ATST learns representations invariant to data augmentation, and BEATs learn from vector quantized representations. They may benefit from learning a representation robust to minor differences in a sound to perform well on these tasks.

3) *Masking Ratio Ablations:* We evaluated the impact of various masking ratios using linear evaluation. Fig. 4 shows the results for the three task groups and the overall average. The best average result (Avg.) was obtained at 0.7. However, the three groups show different trends, indicating that the optimal masking ratio depends on the task. The environmental sound tasks show the best result at 0.8 (or more), while the speech and music tasks have a peak at 0.6 and 0.7, respectively.

We suspect that these optimal masking ratios are due to differences in the density of the target information, as discussed in the MAE paper. The sounds in the speech tasks consist of successive phonemes, making many masks difficult to predict, while the environmental and music tasks include long continuous sounds (e.g., the sound of an air conditioner or long notes of musical instruments), making them easier to predict even at higher masking ratios. The results may indicate that the usefulness of the learned representations for various sounds can be varied and even controlled by masking ratios.

TABLE VI  
EVALUATION IV-C SPECIALIZED REPRESENTATION FOR AUDIOSET: FINE-TUNING RESULTS WITH 95% CI.

Model (/masking ratio), # Params	AS2M mAP	AS20K mAP	ESC-50 acc(%)	SPCV2 acc(%)	VC1 acc(%)
AST (Single)-P/S [19], 86M	45.9	34.7	95.6	98.11	-
HTS-AT [66], 31M	47.1	-	97.0	98.0	-
BEAT <sub>Siter3+</sub> [21], 90M	<b>48.6</b>	<b>41.8</b>	<b>98.1</b>	98.1	-
M2D-AS/0.7, 86M	48.5 ± 0.0	<b>41.8 ± 0.1</b>	97.2 ± 0.1	98.4 ± 0.1	95.6 ± 0.2
<i>(Reference: The M2D model pre-trained in Section IV-B)</i>					
M2D/0.7, 86M	47.9 ± 0.0	38.6 ± 0.1	96.0 ± 0.2	<b>98.4 ± 0.1</b>	<b>96.3 ± 0.2</b>

### C. Evaluation: Specialized Representation for AudioSet

In this experiment, we validated that M2D-X learns an effective representation specializing in AudioSet, conventionally trained in supervised learning using *labels*, such as PANNs [68] and AST [19]. These models demonstrated strong performance for AudioSet and similar tasks such as ESC-50 by learning training signals of multi-label classification with 527 classes. As in the speech domain, these models intensely compete for SOTA AudioSet performance.

We use M2D-X and utilize supervised learning of labels as an additional task in the offline network. Using the configuration in scenario i) from Fig. 3(b), we obtain the predicted logits  $\hat{h}' \in R^{B \times 527}$  transformed by a linear layer with the temporal average pooling of audio features  $\hat{h} \in R^{B \times N_T \times D}$  and calculate the binary cross-entropy (BCE) loss between the  $\hat{h}'$  and the  $\hat{y}$ , which is a multi-hot encoding of the label. The experimental details follow those in Section IV-B, while we used AudioSet labels for pre-training and used only a masking ratio of 0.7, suitable for environmental sound tasks. We did not use the background noise in this experiment. The M2D-X loss weights were set to  $L_{\text{off}} = 1.0$  and  $L_{\text{m2d}} = 1.0$ . We specifically denoted M2D-X with these settings as *M2D-AS*.

1) *Comparison with SOTA models:* The results shown in Tables V and VI compare ours with the AudioSet supervised learning models AST and HTS-AT, plus BEAT<sub>Siter3+</sub>, which used supervised data in SSL similar to ours. M2D-AS improved M2D performance on the target task AudioSet (AS2M, AS20K in Table VI) and ESC-50 in Tables V and VI with results comparable to SOTA models, notably, a close result of AS2M/AS20K with BEAT<sub>Siter3+</sub>, suggesting the performance limit of a similar learning paradigm. The results demonstrate that the M2D-X framework is capable of learning specialized representations for AudioSet with top-level performance.

Unlike previous models, M2D-AS showed the best average result in Table V, demonstrating the general-purpose performance as in M2D. The VC1 result exceptionally dropped by 5.1, but 68.3 % is still a good performance. Other models typi-



cally do not perform at the top level on non-target tasks, such as speech tasks, as shown in our AST/HTS-AT/BEAT<sub>siter3+</sub> results in Table V and our previous study [20]. Our results indicate that combining supervised learning and M2D SSL can achieve specialized and general-purpose performance in a single representation.

In terms of training time, M2D-X can be pre-trained within 2.5 days on 4 A100 GPUs, while BEATs require multiple iterations and 16 GPUs for pre-training.

#### D. Evaluation: Specialized Representation for Speech

In this experiment, we validated that M2D and M2D-X learn effective representations with top-level performance in a highly competitive domain. We pre-trained our models to learn speech representations and compared them with SOTA speech models, expressly HuBERT [9] as a baseline, on the benchmark SUPERB [69].

**Approach.** We first adapted M2D for speech, starting with ablation studies of M2D settings (training dataset, patch size, and input duration) to assess the best M2D performance in this domain.

We then extended M2D to M2D-X to incorporate knowledge learned from the domain techniques for obtaining performance closer to the baseline HuBERT. HuBERT iteratively learns to predict vector-quantized features of masked timesteps, and these target features are a small number (500) of codes in a codebook created by k-means clustering of the features from the previous iteration model. Thus, we assume HuBERT to output clustered target features and distilled HuBERT output features as in the configuration in scenario ii) from Fig. 3(b).

We also used background noise to jointly learn from a denoising task. The conventional method WavLM [11] gains performance by training a denoising task in addition to masked prediction, and we utilized this domain technique. The M2D-X framework provides noisy speech for M2D and clean speech for the offline model, composing a denoising task.

**Pre-training details.** In a distillation configuration of the offline network in M2D-X, we used a linear layer to map the audio feature  $\hat{h} \in R^{B \times N_T \times D}$  to the feature  $\hat{h}' \in R^{B \times N_T \times D_H}$ , a per-time-frame feature, where  $N_T$  is the number of time frames, and  $D_H$  is the feature dimension of HuBERT. We used the ninth transformer layer output of the second-iteration HuBERT Base model<sup>3</sup> as an offline encoder, following WavLM [11], and distilled its output feature  $\hat{y} \in R^{B \times N_T \times D_H}$  using the loss calculation of (2), an MSE with  $l_2$ -normalization.

We used the pre-training settings based on those in Section IV-B with a masking ratio of 0.6, number of epochs to 1000, warm-up epochs to 60, input speech length of 4, 5, and 6 s, and patch size of  $80 \times 2$  and  $80 \times 4$ . We used LibriSpeech [70] with 281,241 samples (960 h) from all training splits (LS-960) for the pre-training dataset. For the background noise dataset, we used AudioSet [28] (AS) with 2,005,132 samples (5569 h). We used M2D-X loss weights of  $L_{\text{off}} = 0.5$  and  $L_{\text{m2d}} = 1.0$ . We denote M2D-X adapted to speech as *M2D-S* (Speech).

<sup>3</sup><https://huggingface.co/facebook/hubert-base-ls960>

TABLE VII  
EVALUATION IV-D SPECIALIZED REPRESENTATION FOR SPEECH:  
DATASET NOISE RATIO ABLATIONS.  
(INPUT DURATION  $T = 2.08$  S AND PATCH SIZE  $80 \times 4$ )

Dataset noise ratio $\eta$	PR PER↓	KS Acc↑	IC Acc↑	SID Acc↑	ER Acc↑	ENV Acc↑	MUS Acc↑
0.0 ( <i>LS-960 only</i> )	<b>10.98</b>	96.85	<b>95.02</b>	74.77	<b>63.02</b>	66.54	49.83
0.1	11.97	97.06	94.38	77.89	61.44	72.77	51.68
0.2	11.87	96.99	93.28	<b>78.46</b>	61.75	73.57	53.76
0.3	12.19	<b>97.23</b>	94.46	78.25	61.55	74.67	54.44
0.4	12.39	97.08	94.15	77.15	61.52	75.16	54.39
0.5	12.53	96.82	92.14	76.58	61.07	76.38	54.73
1.0 ( <i>AudioSet only</i> )	27.04	95.60	82.78	68.54	60.85	<b>83.31</b>	<b>61.88</b>
HuBERT Base [9] <sup>†</sup>	5.41	96.30	98.34	81.42	64.92	62.76	46.26

<sup>†</sup> ENV and MUS results were obtained using publicly available pre-trained models.

TABLE VIII  
EVALUATION IV-D SPECIALIZED REPRESENTATION FOR SPEECH:  
PATCH SIZE ABLATIONS.  
(DATASET NOISE RATIO  $\eta = 0.2$  AND INPUT DURATION  $T = 2.08$  S)

Patch size <i>Freq. × Time</i>	PR PER↓	KS Acc↑	IC Acc↑	SID Acc↑	ER Acc↑	ENV Acc↑	MUS Acc↑
16 × 16 (M2D [26])	77.92	96.36	83.23	79.65	58.88	80.27	59.60
40 × 8	29.28	96.89	89.67	77.51	59.39	78.56	56.62
40 × 4	<b>11.49</b>	96.82	90.93	81.64	60.30	80.00	57.48
40 × 2	15.14	96.79	82.73	<b>85.44</b>	61.49	80.98	58.67
80 × 8	30.28	96.30	90.51	75.66	58.97	72.62	54.28
80 × 4	11.87	96.99	93.28	78.46	<b>61.75</b>	73.57	53.76
80 × 2 (= speech models)	11.74	<b>97.25</b>	<b>93.51</b>	78.86	60.67	74.98	53.28
SSAST-Frame [12]	-	96.7	-	80.8	60.5	-	-
HuBERT Base [9]	5.41	96.30	98.34	81.42	64.92	62.76	46.26

TABLE IX  
EVALUATION IV-D SPECIALIZED REPRESENTATION FOR SPEECH:  
INPUT DURATION ABLATIONS.  
(DATASET NOISE RATIO  $\eta = 0.2$  AND PATCH SIZE  $80 \times 4$ )

Input duration $T$	PR PER↓	KS Acc↑	IC Acc↑	SID Acc↑	ER Acc↑	ENV Acc↑	MUS Acc↑
2.08 s	11.87	96.99	93.28	78.46	61.75	73.57	53.76
3.04 s	9.81	97.09	95.15	79.18	63.39	74.36	52.14
4.00 s	8.50	<b>97.34</b>	94.83	<b>81.24</b>	63.81	74.11	52.23
5.12 s	8.10	97.17	94.70	78.73	<b>65.47</b>	<b>74.69</b>	51.66
6.08 s	<b>7.74</b>	97.17	<b>95.50</b>	80.48	64.06	72.42	50.64
HuBERT Base [9]	5.41	96.30	98.34	81.42	64.92	62.76	46.26

**Evaluation details.** We evaluated models using SUPERB [69] for the speech task performance and conducted a linear evaluation for supplemental assessment of the non-speech performance. In the SUPERB evaluation, the model weights were frozen, and the weighted sum of the features from all transformer layers was used in the evaluation. We standardized spectrograms with statistics of the dataset of each SUPERB task. The evaluation tasks included phoneme recognition (PR), keyword spotting (KS), intent classification (IC), speaker identification (SID), and emotion recognition (ER); we chose them to form a balanced subset from each speaker/content/semantics/paralinguistics subcategories listed in Table I from WavLM [11]. In addition, we also tested models on automatic speaker verification (ASV) in Table X. For the linear evaluation, we used the same setup as in Section IV-B and assessed the average accuracies of two environmental sound tasks (ENV) and three music tasks (MUS). Note that, unlike SUPERB, the linear evaluation used only the final layer features of the frozen model.

TABLE X  
EVALUATION IV-D SPECIALIZED REPRESENTATION FOR SPEECH: COMPARISON WITH SOTA SPEECH MODELS.

Model (/masking ratio)	# Params Million	Dataset	PR PER↓	KS Acc↑	IC Acc↑	SID Acc↑	ASV EER↓	ER Acc↑	ENV Acc↑	MUS Acc↑
<i>(SOTA models)</i>										
wav2vec2.0 Base [8]†	95M	LS-960	5.74	96.23	92.35	75.18	6.02	63.43	37.66	32.02
WavLM Base [11]†	95M	LS-960+DNS	<b>4.84</b>	96.79	<b>98.63</b>	<b>84.51</b>	<b>4.69</b>	65.94	54.45	40.98
HuBERT Base [9]† ( <i>Baseline</i> )	95M	LS-960	5.41	96.30	98.34	81.42	5.11	64.92	62.76	46.26
<i>(Ours: M2D-S with <math>\lambda_{off} = 0.5</math>, <math>\lambda_{m2d} = 1</math>, <math>\eta = 0.2</math>, and patch size <math>80 \times 2</math>)</i>										
M2D-S/0.6 T=4.0s	86M	LS-960+AS	5.72	96.47	97.80	81.97	6.29	<b>66.36</b>	53.22	41.71
M2D-S/0.6 T=5.12s	86M	LS-960+AS	5.64	96.87	97.65	80.69	7.07	65.35	57.34	43.23
M2D-S/0.6 T=6.08s	86M	LS-960+AS	5.33	96.80	97.63	81.74	5.97	66.13	54.77	43.75
<i>(Reference: M2D with setting modifications only, <math>\eta = 0.2</math>, and patch size <math>80 \times 4</math>)</i>										
M2D/0.6 T=4.00s	86M	LS-960+AS	8.50	<b>97.34</b>	94.83	81.24	7.13	63.81	74.11	52.23
M2D/0.6 T=5.12s	86M	LS-960+AS	8.10	97.17	94.70	78.73	7.15	65.47	74.69	51.66
M2D/0.6 T=6.08s	86M	LS-960+AS	7.74	97.17	95.50	80.48	6.84	64.06	72.42	50.64
<i>(Reference: The M2D model pre-trained in Section IV-B) *ASV test fails with the patch size <math>16 \times 16</math>.</i>										
M2D/0.6, T=6.08s, patch size $16 \times 16$	86M	AS	78.30	95.65	76.77	80.68	N/A	61.17	<b>88.63</b>	<b>66.56</b>
<i>(Reference: Previous similar study using ViT-based Base model)</i>										
SSAST-Frame [12]	89M	LS-960 $\cup$ AS‡	-	96.7	-	80.8	-	60.5	-	-
SSAST-Patch [12]	89M	LS-960 $\cup$ AS‡	-	94.8	-	57.1	-	56.8	-	-

† ENV and MUS results were obtained using publicly available pre-trained models.

‡ The LS-960 and AS samples were used without mixing one as background noise into others, unlike M2D-S.

1) *Adapting M2D to Speech:* We adapted the M2D settings for the speech tasks. In the following ablation studies, we sought the best parameter with the defaults: dataset noise ratio of 0.2, input duration of 2.08 s, and patch size of  $80 \times 4$ .

**Pre-training dataset ablations.** We assessed the impact of datasets on pre-training by changing the dataset noise ratio  $\eta$  to control the mixing of the target data LibriSpeech and the background noise AudioSet, and we set  $\lambda_{off} = 0$ . When using AudioSet only, we defined one epoch as the number of LibriSpeech samples, and we randomly sampled from AudioSet.

The results in Table VII show that the speech tasks perform best when using only LibriSpeech, and performance deteriorates as the ratio of AudioSet increases. Conversely, the non-speech tasks (ENV, MUS) perform best when using only AudioSet, and performance deteriorates as the ratio of LibriSpeech increases. Except for SID, which performed best at around  $\eta = 0.2$ , using a speech dataset only performs better in speech tasks.

Note that many AudioSet samples contain speech. While the speech quality is typically bad compared to a speech corpus, it may provide a performance boost when used with LibriSpeech.

**Patch size ablations.** We examined the impact on the performance of the patch splitting of the input spectrogram, which is a key difference between the general-purpose model and the speech model. The results in Table VIII indicate that the setting equivalent to the speech model ( $80 \times 2$ ) has the best performance balance except for SID; for patch size  $80 \times 2$  (Frequency  $\times$  Time-step), 80 indicates no splitting on the frequency axis, and 2 corresponds to 20 ms per frame. Notably, this result aligns with SSAST [12] using a similar patch size of  $128 \times 2$ . While  $40 \times 2$  performs the best on SID, it significantly degrades on PR and IC. The results also show that the longer time steps (lower frame rates) degrade the performance, especially in PR, similar to the results in [71].

**Input duration ablations.** Table IX shows that increasing the input duration brings the performance closer to the baseline HuBERT. These results show that while the performance on

TABLE XI  
EVALUATION IV-D SPECIALIZED REPRESENTATION FOR SPEECH: PRE-TRAINING TASK ABLATIONS. (INPUT DURATION  $T = 2.08$  S, AND PATCH SIZE  $80 \times 4$ )

	Offline		Online	PR	KS	IC	SID	ER	ENV	MUS
	denoise	distill	M2D	PER↓	Acc↑	Acc↑	Acc↑	Acc↑	Acc↑	Acc↑
(a)			✓	11.87	<b>96.99</b>	93.28	<b>78.46</b>	61.75	73.57	53.76
(b)		✓		8.10	96.05	94.81	65.51	61.27	56.96	44.16
(c)	✓	✓		7.80	94.66	93.38	70.03	61.58	42.42	35.36
(d)		✓	✓	8.78	95.72	91.35	62.68	<b>60.85</b>	57.15	43.75
(e)	✓	✓	✓	<b>7.02</b>	95.48	<b>97.10</b>	78.12	<b>64.09</b>	55.49	41.51

KS, SID, and ER reached the same level as HuBERT, it is difficult to approach that level of performance on PR and IC.

2) *Comparison with SOTA Models:* With the best parameters in the previous section, we extended M2D to M2D-S to assess further performance gain, especially on PR and IC, using the speech domain techniques. M2D-S learns from a multi-task of M2D, distilling HuBERT features for learning clustered features and denoising as in WavLM. Table X summarizes the results of M2D-S, M2D, and SOTA models.

The table shows M2D-S results comparable to HuBERT except for IC and ASV, with a performance gap of  $-0.54$  to  $-0.71$  on IC and  $-0.86$  to  $-1.96$  on ASV. Compared to wav2vec2.0, M2D-S results are better except for ASV, for which they are comparable. Compared to WavLM, M2D-S performed worse with gaps on PR of  $-0.49$  to  $-0.88$ , IC of  $-0.83$  to  $-1.0$ , SID of  $-2.54$  to  $-3.82$ , and ASV of  $-1.28$  to  $-2.38$ . While M2D-S learns from a denoising task as in WavLM, we did not observe a performance boost such as WavLM’s SID with 84.51, suggesting the M2D-S’s denoising did not work as well as WavLM’s.

Overall, M2D-S performed better than wav2vec2.0 and closer to HuBERT. However, it did not show robust results, especially on ASV, and performed worse than WavLM. Although the M2D-S results were not comparable with all speech model results, the comparison among M2D-S, wav2vec2.0, and HuBERT indicated that M2D-S achieved learning a domain representation with top-level performance.

**Pre-training task ablations.** We further assessed the contribution of the tasks learned in M2D-S. We switched the tasks

in the offline and M2D networks by setting  $\lambda_{\text{off}}$  and  $\lambda_{\text{m2d}}$  in (6) to 0 or 1.0, respectively, and switched the denoising task by setting  $\eta$  to 0 (disabled) or 0.2 (enabled).

The results in Table XI show that (b) distillation only is better than (a) M2D or (d) M2D plus distillation, indicating that the distillation of a speech model trained with clustered features is effective. Compared to (b) with only distillation, (c) with additional denoising performs better except for KS and IC, indicating the effectiveness of the denoising task. M2D-S configuration (e) shows that learning all tasks together effectively improves performance.

### E. Evaluation: Specialized Representation for Medical Application

This experiment simulated cases of private and proprietary data, where the data size is typically limited and its distribution differs from a large pre-training dataset; we validated our models for learning a specialized representation with top-level performance in these cases. We used the Respiratory Sound Database from ICBHI (International Conference on Biomedical and Health Informatics) 2017 Challenge (ICBHI2017) [72], a dataset from the medical field for evaluating respiratory sound classification algorithms, containing only 920 recordings (5.5 h) for 128 subjects. Since pre-training with masked prediction usually requires a large dataset [24], [25], pre-training on a small amount of data is challenging. We tried to pre-train an M2D using only ICBHI2017 in a preliminary evaluation; however, as shown in Table XII(2), it underperformed the randomly initialized models, confirming that the pre-training had failed.

To facilitate the assessment of the contribution of pre-training, we used a codebase from Moummad et al. [73], in which we only replaced the encoder that extracts the audio features. This codebase uses PANNs [68] pre-trained models as an encoder and is suitable for comparison. Solutions of the codebase use Supervised Contrastive Learning (SCL) [74] and learning based on Cross Entropy (CE) loss for the fine-tuning algorithm; we used only the CE loss for ease of comparison.

We also limited the computational and data resources in the experiments to assess the applicability to a real-world scenario. We used a single GPU with 24 GB of memory (e.g., NVIDIA GeForce RTX 3090 Ti) for pre-training and subsequent fine-tuning and FSD50K [75] for background noise, which is practical in terms of availability and size while providing a wide variety of sounds. We also set a goal of completing the pre-training and fine-tuning within a day for each.

**Approach.** We adopted a *further pre-training* [45] strategy, which pre-trains a pre-trained model once again, using M2D-X on the target dataset ICBHI2017.

In the further pre-training of M2D-X, we used the configuration in scenario iii) from Fig. 3(b), employing the M2D model pre-trained on AudioSet as the offline teacher model and as the initial M2D online encoder weights. The combination of the data augmentation effect and denoising task brought by the use of background noise promotes an effective representation, and distilling the features from the frozen AudioSet pre-trained

TABLE XII  
EVALUATION IV-E SPECIALIZED REPRESENTATION FOR ICBHI2017:  
PRILIMINARY EVALUATION RESULTS WITH 95% CI.

Model (/masking ratio)	Sp	Se	Score
<i>(1) Patch size/masking ratio ablations</i>			
16×16/0.6 (T=6.08s)	77.67 ± 1.82	42.54 ± 1.59	60.10 ± 0.37
16×16/0.7 (T=6.08s)	79.47 ± 2.10	42.93 ± 1.84	61.20 ± 0.46
80×4/0.7 (T=6.08s)	<b>79.52 ± 1.44</b>	40.22 ± 1.43	59.87 ± 0.28
16×4/0.7 (T=2.00s)	79.48 ± 1.47	<b>44.38 ± 1.55</b>	<b>61.93 ± 0.25</b>
<i>(2) Pre-training ablations</i>			
No pre-training (random initial weights)	57.02 ± 9.61	32.39 ± 5.71	44.71
M2D pre-training on ICBHI2017 only	45.36 ± 5.55	38.29 ± 3.52	41.83

model regularizes learned features from overfitting to the small target dataset ICBHI2017.

We also evaluated further pre-training of M2D by setting  $L_{\text{off}} = 0$  in M2D-X, in addition to M2D-X configuration, to assess the contribution of the regularization.

**Further pre-training details.** Based on the preliminary experiments shown in Table XII(1), we used the AudioSet pre-trained M2D model with a patch size of  $16 \times 4$ , input audio duration of 2.0 s, and masking ratio of 0.7. We used this model as an offline teacher and also as the initial online encoder weights. We used the M2D-X offline network based on the distillation configuration in Section IV-D and additionally reshaped the offline teacher output using (4) to obtain the training signal per timestep  $\tilde{y} \in R^{B \times N_T \times D}$ . We set the M2D-X loss weights  $L_{\text{m2d}}$  and  $L_{\text{off}}$  to 1.0.

While we used 539 ICBHI training samples, we virtually increased samples by replicating the data list and rounding fractions to 10,000 samples, treated as one epoch, to make the training process manageable. We used FSD50K as background noise and set the  $\eta$  to 0.3. To train on a 24 GB GPU, we set the batch size to 64 and the gradient accumulation [76] to two iterations (effective batch size of 128). We used the same learning rate and EMA decay as in Section IV-A. We pre-trained 600 epochs with 24 warm-up epochs and saved and evaluated checkpoints every 100 epochs.

**Fine-tuning evaluation details.** For stable experimental results, we fixed the learning rate to 0.00005 and the batch size to 64 and trained 150 epochs. To accommodate execution on a small GPU, we minimally modified the codebase to allow for gradient accumulation, and the mini-batch was split into four during inference. ICBHI2017 consists of 4142 training and 2756 test samples, for a total of 6898 sample respiratory cycles cropped from 539 training and 381 test recordings. We evaluated it with a standard four-class classification task and compared models using the ICBHI2017 test metrics of Sensitivity (Se), Specificity (Sp), and Score, which is the average of Se and Sp. We use Score as the primary metric for comparison. Due to the high variability of the results, we averaged with 95% CI the 20 results obtained by fine-tuning each of the four pre-trained models five times.

*1) Comparison with SOTA Models:* Table XIII compares the results. For the (i) original M2D results, the default patch size  $16 \times 16$  of 61.20 outperforms the CE model of Bae&Kim et al. [77] of 59.55 and Moummad et al. [73] results. Bae&Kim et al. and Moummad et al. used AST [19] and PANNs CNN6 [68] trained by supervised learning of AudioSet. The results

TABLE XIII

EVALUATION IV-E SPECIALIZED REPRESENTATION FOR ICBHI2017: COMPARISON WITH SOTA MODELS WITH 95% CI.

Model (/masking ratio)	Backbone	Sp	Se	Score
<i>(Baseline models with 4.3M params)</i>				
Moummad et al. (CE) [73]	CNN6 [68]	70.09	40.39	55.24
Moummad et al. (SCL) [73]	CNN6 [68]	75.95	39.15	57.55
<i>(SOTA models with 86M params)</i>				
Bae&Kim et al. (CE) [77]	AST [19]	77.14	41.97	59.55
Bae&Kim et al. (MixCL) [77]	AST [19]	<b>81.66</b>	43.07	62.37
<i>(i) Ours: Original M2D (pre-trained on AudioSet only) with 86M params</i>				
M2D/0.7 (16×16, T=6.08s)	M2D ViT	79.47 ± 2.10	42.93 ± 1.84	61.20 ± 0.46
M2D/0.7 (16×4, T=2.0s)	M2D ViT	79.48 ± 1.47	44.38 ± 1.55	61.93 ± 0.25
<i>(ii) Ours: further pre-trained on ICBHI2017 (16×4, T=2.0s) with 86M params</i>				
M2D/0.7 (η = 0.3)	M2D ViT	80.70 ± 1.66	44.76 ± 1.50	62.73 ± 0.30
M2D-X/0.7 (η = 0.3)	M2D ViT	81.51 ± 1.03	45.08 ± 1.10	<b>63.29 ± 0.22</b>
<i>(iii) Ablations: further pre-trained without BG noise data (16×4, T=2.0s) with 86M params</i>				
M2D/0.7 (η = 0.0)	M2D ViT	78.66 ± 1.60	43.67 ± 1.49	61.17 ± 0.35
M2D-X/0.7 (η = 0.0)	M2D ViT	77.39 ± 1.69	<b>46.04 ± 1.66</b>	61.71 ± 0.34

suggest that ICBHI2017 has a different data distribution from AudioSet and that the M2D representation learned by SSL is more applicable to the task than supervised learning representations. Meanwhile, Bae&Kim et al. (MixCL) outperforms M2D with a SOTA score of 62.37, which uses the fine-tuning algorithm Patch-Mix Contrastive Learning (MixCL), showing the effectiveness of the fine-tuning technique for the task. M2D patch size 16 × 4 improves performance to 61.93, but it still underperforms Bae&Kim et al. (MixCL).

The (ii) results show that further pre-training improves the performance of our models to outperform SOTA, and M2D-X improves performance even more. The M2D/0.7 (η = 0.3) result of 62.73 outperforms the SOTA by 0.36, while the M2D-X/0.7 (η = 0.3) result of 63.29 outperforms SOTA by 0.92. The difference between M2D-X and M2D (M2D-X with L<sub>off</sub> = 0) indicates the regularization in the offline network contributes to gaining the performance from 62.73 to 63.29.

Overall, these results show that M2D and M2D-X learn top-level representations even on a small target dataset under a further pre-training setting.

2) *Background Noise Ablations:* We assessed the performance contribution of the use of background noise data.

The (iii) ablations without background noise data show that both M2D and M2D-X further pre-training degrades, resulting in worse performance. In particular, the result for M2D/0.7 (η = 0.0) is 61.17, degraded by 0.76 from 61.93 before further pre-training. On the other hand, the result for M2D-X/0.7 (η = 0.0) was 61.71, showing a smaller decline by 0.22 from 61.93, confirming the effect of the regularization task in preventing the representations from overfitting.

Sun et al. [45] have reported that in the NLP domain, further pre-training on a small target dataset does harm, but that it is effective on a sufficiently large dataset of the same domain. In M2D-X, we think that the effect of data augmentation through the use of background noise works similarly to the use of a dataset of the same domain with a larger size.

Overall, the offline network introduced in M2D-X indicates the effect of preventing overfitting, and the use of background noise suggests the effect of data augmentation, demonstrating that the M2D-X framework is effective for learning representations in the experimental scenarios.

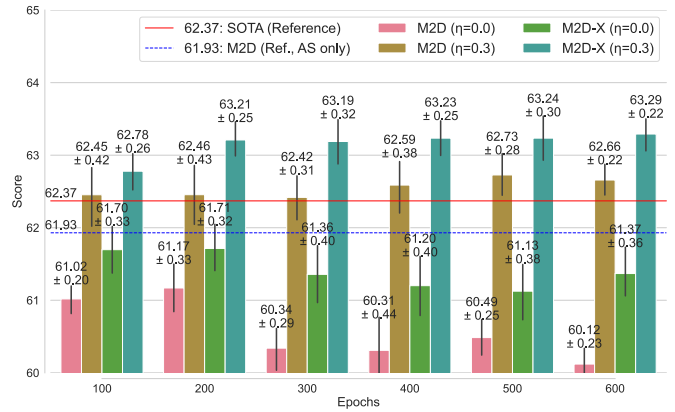


Fig. 5. Evaluation IV-E Specialized Representation for ICBHI2017: Comparing the progress of Score (%) among further pre-training settings.

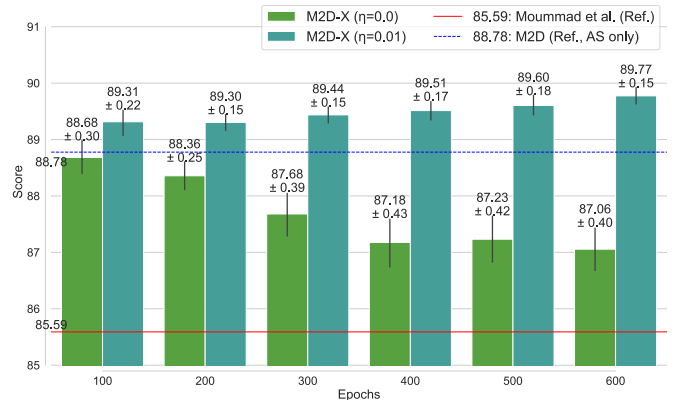


Fig. 6. Evaluation IV-E Dataset Ablation using SPRSound: Comparing the progress of Score (%).

3) *Performance Transition in Training Progress:* We evaluated the performance of checkpoints saved during the training process as shown in Fig. 5. The graph shows that when background noise is used (η = 0.3), the performance improves with the progress of the training process. On the other hand, when background noise is not used (η = 0.0), performance deteriorates with progress, indicating that the learned representations become less useful as epoch progresses.

These results show that introducing background noise changed the performance of learned representations from deteriorating with progress to improving for both M2D and M2D-X. Focusing on the performance change, the improvement for M2D begins after 400 epochs, whereas for M2D-X, it begins earlier, at 200 epochs. In addition, M2D-X shows more significant performance gains, indicating that it can effectively achieve further pre-training in a small-data scenario with the help of the background noise and additional tasks.

4) *Dataset Ablation using SPRSound:* We further verified the applicability of M2D-X to another dataset using SPRSound [78], a dataset similar to ICBHI2017. SPRSound is a respiratory sound dataset comprising 2683 recordings (8.2 h) from 292 subjects and is as small as ICBHI2017 (920 recordings/5.5 h/128 subjects). We used the inter-patient test split as in [73]. We set the background noise ratio to 0.01 for pre-training, the learning rate to 5 × 10<sup>-6</sup>, and the training epochs to 50 for fine-tuning. Other experimental details are the same as in the experiment using ICBHI2017.

As shown in Fig. 6, we observe behavior similar to that in the ICBHI2017 experiment. When background noise is not used ( $\eta = 0$ ), the performance deteriorates as progress proceeds, but it improves when the noise is used ( $\eta = 0.01$ ). Compared to the baseline, Moummad et al. [73], our results are higher than their result of 85.59 with the highest result of 89.77. In summary, we confirmed that our models also achieve top-level performance on SPRSound, and M2D-X benefits from the background noise for successful further pre-training on a small dataset.

## V. CONCLUSION

This paper proposed M2D, a masked prediction-based SSL, and M2D-X, extending M2D to a universal audio pre-training framework. M2D improved performance by using only masked patches to obtain training signals, unlike previous methods that use all patches. M2D-X extends M2D by adding an extra learning task and background noise data, enabling pre-training of representations specialized for an application even when data size is small and the distribution is different from that public audio datasets, as typically found in private and proprietary cases.

Our experiments confirmed that M2D and M2D-X learn effective representations, including a general-purpose audio representation, specialized representations for the highly competitive AudioSet and speech domain, and a specialized representation for a medical application with small data. These representations all achieved top-level performance, demonstrating their potential for use as a universal framework to provide effective audio pre-training for diverse applications.

We found that encoding only the masked parts of the input to obtain a training signal improves the average performance of the masked prediction-based SSL, that a multi-task of supervised learning and M2D SSL enhances specialized performance on top of the general-purpose performance, and that M2D-X configured for regularization using background noise enables successful further pre-training on small data.

As a practical example, we presented small-data medical application experiments using only a single GPU. We hope that the published code and AudioSet pre-trained models, as well as the example, will enable pre-training and improve performance in future audio studies<sup>4</sup>. Future work may include studies that guide the data selection, post-training model selection, and hyperparameter settings, such as downstream task performance estimation using validation loss [24], [79].

## APPENDIX A EXPERIMENT WITH IMAGES

Since M2D accepts general 2D structural data input, we validated the effectiveness of M2D for images through a standard performance evaluation using ImageNet [80]. We pre-trained on ImageNet-1K, followed by fine-tuning. The results showed top-1 validation accuracy for a single crop image of  $224 \times 224$ , the same as in the MAE [3].

<sup>4</sup>Codes, pre-trained weights, and examples are available at: <https://github.com/nttclsab/m2d>

TABLE XIV  
FINE-TUNING RESULTS ON IMAGENET-1K.

Model	Target encoder	Target input	Top-1 acc(%)
MAE		-	83.22 $\pm$ 0.024
M2D variant (conventional)	✓	All patches	83.22 $\pm$ 0.085
M2D (ours)	✓	Masked patches only	<b>83.35</b> $\pm$ 0.211

TABLE XV  
REQUIRED RESOURCES FOR PRE-TRAINING OR FURTHER PRE-TRAINING

Training type and settings						Resources	
PT* /Fur-PT	Input dur.	Patch size	Epochs	Batch size	Grad. accum.	Training time (h)	GPU usage
<i>Section IV-B M2D for General-purpose</i>							
PT	6 s	16 $\times$ 16	300	512	1	55	4 $\times$ A100 80GB
<i>Section IV-C M2D-X for AudioSet</i>							
PT	6 s	16 $\times$ 16	300	512	1	55	4 $\times$ A100 80GB
<i>Section IV-D M2D-X for Speech</i>							
PT	4 s	80 $\times$ 2	1000	512	1	56	4 $\times$ A100 80GB
PT	5 s	80 $\times$ 2	1000	256	2	65	4 $\times$ A100 80GB
PT	6 s	80 $\times$ 2	1000	256	2	77	4 $\times$ A100 80GB
<i>Section IV-E M2D-X for ICBHI2017</i>							
PT	2 s	16 $\times$ 4	300	512	1	109	4 $\times$ A100 80GB
Fur-PT	2 s	16 $\times$ 4	600	64	2	7	1 $\times$ RTX 3090 Ti

\* Pre-training (PT) or further pre-training (Fur-PT).

We used the MAE code as a base, as in Section IV-A, and made minimal changes to it, allowing comparison of differences only in the experimental subjects of interest. We also used ViT-Base [17] for the backbone. For pre-training, we set the number of epochs as 300 and the batch size as 2048. All other settings were the same as in the MAE, including the masking ratio of 0.75. The EMA decay rate  $\tau$  was the same as in Section IV-A. For fine-tuning, we used the same code and parameters as in the MAE.

We compared three models, MAE, M2D, and an M2D variant, that feed all patches to the target encoder. Table XIV shows the results. The results show that the performance of the M2D variant with all patches input to the target, which is conventional, is comparable to MAE, and that our M2D outperforms these methods, validating that our method is also effective on images in addition to audio.

## APPENDIX B COMPUTATIONAL RESOURCES FOR PRE-TRAINING

We show the details of the required computational resources for the pre-training for each experiment in Table XV. The effective batch size for all pre-training is 2048, and it is 128 for additional pre-training.

## REFERENCES

- [1] J. Devlin, M. Chang, K. Lee, and K. Toutanova, "BERT: pre-training of deep bidirectional transformers for language understanding," in *NAACL-HLT*, 2019, pp. 4171–4186.
- [2] Y. Liu, M. Ott, N. Goyal, J. Du, M. Joshi, D. Chen, O. Levy, M. Lewis, L. Zettlemoyer, and V. Stoyanov, "RoBERTa: A Robustly Optimized BERT Pretraining Approach," *arXiv preprint arXiv:1907.11692*, 2019.
- [3] K. He, X. Chen, S. Xie, Y. Li, P. Dollár, and R. Girshick, "Masked Autoencoders Are Scalable Vision Learners," in *CVPR*, June 2022, pp. 16 000–16 009.
- [4] C. Tao, X. Zhu, W. Su, G. Huang, B. Li, J. Zhou, Y. Qiao, X. Wang, and J. Dai, "Siamese Image Modeling for Self-Supervised Vision Representation Learning," in *CVPR*, Jun 2023, pp. 2132–2141.

- [5] M. Assran, M. Caron, I. Misra, P. Bojanowski, F. Bordes, P. Vincent, A. Joulin, M. Rabbat, and N. Ballas, “Masked Siamese Networks for Label-Efficient Learning,” in *ECCV*, 2022, p. 456–473.
- [6] X. Chen, M. Ding, X. Wang, Y. Xin, S. Mo, Y. Wang, S. Han, P. Luo, G. Zeng, and J. Wang, “Context Autoencoder for Self-Supervised Representation Learning,” *Int. J. Comput. Vis.*, pp. 208–223, 2024.
- [7] A. El-Nouby, G. Izacard, H. Touvron, I. Laptev, H. Jegou, and E. Grave, “Are Large-scale Datasets Necessary for Self-Supervised Pre-training?” *arXiv preprint arXiv:2112.10740*, 2021.
- [8] A. Baevski, Y. Zhou, A. Mohamed, and M. Auli, “wav2vec 2.0: A Framework for Self-Supervised Learning of Speech Representations,” in *NeurIPS*, 2020.
- [9] W.-N. Hsu, B. Bolte, Y.-H. H. Tsai, K. Lakhota, R. Salakhutdinov, and A. Mohamed, “HuBERT: Self-Supervised Speech Representation Learning by Masked Prediction of Hidden Units,” *IEEE/ACM Trans. Audio, Speech, Language Process.*, vol. 29, p. 3451–3460, 2021.
- [10] A. Conneau, A. Baevski, R. Collobert, A. Mohamed, and M. Auli, “Un-supervised Cross-Lingual Representation Learning for Speech Recognition,” in *Interspeech*, 2021, pp. 2426–2430.
- [11] S. Chen, C. Wang, Z. Chen, Y. Wu, S. Liu, Z. Chen, J. Li, N. Kanda, T. Yoshioka, X. Xiao, J. Wu, L. Zhou, S. Ren, Y. Qian, Y. Qian, J. Wu, M. Zeng, X. Yu, and F. Wei, “WavLM: Large-Scale Self-Supervised Pre-Training for Full Stack Speech Processing,” *IEEE J. Sel. Top. Signal Process.*, vol. 16, no. 6, p. 1505–1518, 2022.
- [12] Y. Gong, C.-I. Lai, Y.-A. Chung, and J. Glass, “SSAST: Self-Supervised Audio Spectrogram Transformer,” in *AAAI*, vol. 36, no. 10, 2022, pp. 10 699–10 709.
- [13] P.-Y. Huang, H. Xu, J. Li, A. Baevski, M. Auli, W. Galuba, F. Metze, and C. Feichtenhofer, “Masked autoencoders that listen,” in *NeurIPS*, 2022.
- [14] A. Baade, P. Peng, and D. Harwath, “MAE-AST: Masked Autoencoding Audio Spectrogram Transformer,” in *Interspeech*, 2022, pp. 2438–2442.
- [15] D. Chong, H. Wang, P. Zhou, and Q. Zeng, “Masked Spectrogram Prediction For Self-Supervised Audio Pre-Training,” in *ICASSP*, 2023, pp. 1–5.
- [16] D. Niizumi, D. Takeuchi, Y. Ohishi, N. Harada, and K. Kashino, “Masked Spectrogram Modeling using Masked Autoencoders for Learning General-purpose Audio Representation,” in *HEAR: Holistic Evaluation of Audio Representations (NeurIPS 2021 Competition)*, vol. 166, 2022, pp. 1–24.
- [17] A. Dosovitskiy, L. Beyer, A. Kolesnikov, D. Weissenborn, X. Zhai, T. Unterthiner, M. Dehghani, M. Minderer, G. Heigold, S. Gelly, J. Uszkoreit, and N. Houlsby, “An image is worth 16x16 words: Transformers for image recognition at scale,” in *ICLR*, 2021.
- [18] A. Baevski, W.-N. Hsu, Q. Xu, A. Babu, J. Gu, and M. Auli, “data2vec: A General Framework for Self-supervised Learning in Speech, Vision and Language,” in *ICML*, 2022, pp. 1298–1312.
- [19] Y. Gong, Y.-A. Chung, and J. Glass, “AST: Audio Spectrogram Transformer,” in *Interspeech*, 2021, pp. 571–575.
- [20] D. Niizumi, D. Takeuchi, Y. Ohishi, N. Harada, and K. Kashino, “BYOL for Audio: Exploring Pre-trained General-purpose Audio Representations,” *IEEE/ACM Trans. Audio, Speech, Language Process.*, vol. 31, p. 137–151, 2023.
- [21] S. Chen, Y. Wu, C. Wang, S. Liu, D. Tompkins, Z. Chen, and F. Wei, “BEATs: Audio Pre-Training with Acoustic Tokenizers,” in *ICML*, 2023.
- [22] J. Peng, T. Stafylakis, R. Gu, O. Plhot, L. Mošner, L. Burget, and J. Černocký, “Parameter-Efficient Transfer Learning of Pre-Trained Transformer Models for Speaker Verification Using Adapters,” in *ICASSP*, 2023, pp. 1–5.
- [23] T. Ashihara, T. Moriya, K. Matsuura, and T. Tanaka, “Exploration of Language Dependency for Japanese Self-Supervised Speech Representation Models,” in *ICASSP*, 2023, pp. 1–5.
- [24] Z. Xie, Z. Zhang, Y. Cao, Y. Lin, Y. Wei, Q. Dai, and H. Hu, “On Data Scaling in Masked Image Modeling,” in *CVPR*, June 2023, pp. 10 365–10 374.
- [25] C. Zhang, C. Zhang, J. Song, J. S. K. Yi, and I. S. Kweon, “A Survey on Masked Autoencoder for Visual Self-supervised Learning,” in *IJCAI*, Aug 2023, pp. 6805–6813.
- [26] D. Niizumi, D. Takeuchi, Y. Ohishi, N. Harada, and K. Kashino, “Masked Modeling Duo: Learning Representations by Encouraging Both Networks to Model the Input,” in *ICASSP*, 2023, pp. 1–5.
- [27] —, “Masked Modeling Duo for Speech: Specializing General-Purpose Audio Representation to Speech using Denoising Distillation,” in *Interspeech*, 2023, pp. 1294–1298.
- [28] J. F. Gemmeke, D. P. W. Ellis, D. Freedman, A. Jansen, W. Lawrence, R. C. Moore, M. Plakal, and M. Ritter, “Audio Set: An ontology and human-labeled dataset for audio events,” in *ICASSP*, 2017, pp. 776–780.
- [29] D. S. Park, W. Chan, Y. Zhang, C.-C. Chiu, B. Zoph, E. D. Cubuk, and Q. V. Le, “SpecAugment: A Simple Data Augmentation Method for Automatic Speech Recognition,” in *Interspeech*, 2019, pp. 2613–2617.
- [30] J.-B. Grill, F. Strub, F. Altché, C. Tallec, P. H. Richemond, E. Buchatskaya, C. Doersch, B. A. Pires, Z. D. Guo, M. G. Azar, B. Piot, K. Kavukcuoglu, R. Munos, and M. Valko, “Bootstrap Your Own Latent - A New Approach to Self-Supervised Learning,” in *NeurIPS*, 2020.
- [31] A. T. Liu, S.-w. Yang, P.-H. Chi, P.-c. Hsu, and H.-y. Lee, “Mockingjay: Unsupervised Speech Representation Learning with Deep Bidirectional Transformer Encoders,” in *ICASSP*, 2020, pp. 6419–6423.
- [32] A. T. Liu, S.-W. Li, and H.-y. Lee, “TERA: Self-Supervised Learning of Transformer Encoder Representation for Speech,” *IEEE/ACM Trans. Audio, Speech, Language Process.*, vol. 29, pp. 2351–2366, 2021.
- [33] Y. Zhang, D. S. Park, W. Han, J. Qin, A. Gulati, J. Shor, A. Jansen, Y. Xu, Y. Huang, S. Wang, Z. Zhou, B. Li, M. Ma, W. Chan, J. Yu, Y. Wang, L. Cao, K. C. Sim, B. Ramabhadran, T. N. Sainath, F. Beaufays, Z. Chen, Q. V. Le, C.-C. Chiu, R. Pang, and Y. Wu, “BigSSL: Exploring the frontier of large-scale semi-supervised learning for automatic speech recognition,” *IEEE J. Sel. Top. Signal Process.*, vol. 16, no. 6, p. 1519–1532, 2022.
- [34] Z. Ma, Z. Zheng, C. Tang, Y. Wang, and X. Chen, “MT4SSL: Boosting Self-Supervised Speech Representation Learning by Integrating Multiple Targets,” in *Interspeech*, 2023, pp. 82–86.
- [35] J.-S. Choi, J.-H. Lee, C.-W. Lee, and J.-H. Chang, “M-CTRL: A Continual Representation Learning Framework with Slowly Improving Past Pre-Trained Model,” in *ICASSP*, 2023, pp. 1–5.
- [36] H.-J. Chang, S.-w. Yang, and H.-y. Lee, “DistilHuBERT: Speech Representation Learning by Layer-wise Distillation of Hidden-unit BERT,” in *ICASSP*, 2022, pp. 7087–7091.
- [37] H. Wang, Y. Qian, X. Wang, Y. Wang, C. Wang, S. Liu, T. Yoshioka, J. Li, and D. Wang, “Improving Noise Robustness of Contrastive Speech Representation Learning with Speech Reconstruction,” in *ICASSP*, 2022, pp. 6062–6066.
- [38] H. R. Guimarães, A. Pimentel, A. R. Avila, M. Rezagholizadeh, B. Chen, and T. H. Falk, “RobustDistiller: Compressing Universal Speech Representations for Enhanced Environment Robustness,” in *ICASSP*, 2023.
- [39] X. Li and X. Li, “ATST: Audio Representation Learning with Teacher-Student Transformer,” in *Interspeech*, 2022, pp. 4172–4176.
- [40] L. Wang, P. Luc, Y. Wu, A. Recasens, L. Smaira, A. Brock, A. Jaegle, J.-B. Alayrac, S. Dieleman, J. Carreira, and A. van den Oord, “Towards Learning Universal Audio Representations,” in *ICASSP*, 2022, pp. 4593–4597.
- [41] S. Ghosh, A. Seth, and S. Umesh, “Decorrelating Feature Spaces for Learning General-Purpose Audio Representations,” *IEEE J. Sel. Topics Signal Process.*, vol. 16, no. 6, pp. 1402–1414, 2022.
- [42] L. Melms, R. R. Ilesan, U. Köhler, O. Hildebrandt, R. Conrath, J. Eckstein, C. Atila, S. Matrood, B. Schieffer, J. R. Schaefer, T. Müller, J. Obergassel, N. Schlicker, and M. C. Hirsch, “Training one model to detect heart and lung sound events from single point auscultations,” *arXiv preprint arXiv:2301.06078*, 2023.
- [43] N. Scheidwasser-Clow, M. Kegler, P. Beckmann, and M. Cernak, “SERAB: A Multi-Lingual Benchmark for Speech Emotion Recognition,” in *ICASSP*, 2022, pp. 7697–7701.
- [44] A. Lauscher, I. Vulić, E. M. Ponti, A. Korhonen, and G. Glavaš, “Specializing Unsupervised Pretraining Models for Word-Level Semantic Similarity,” in *COLING*, 2020, pp. 1371–1383.
- [45] C. Sun, X. Qiu, Y. Xu, and X. Huang, “How to Fine-Tune BERT for Text Classification?” in *CCL*, 2019, pp. 194–206.
- [46] Q. Zhu, Y. Gu, L. Luo, B. Li, C. Li, W. Peng, M. Huang, and X. Zhu, “When does further pre-training MLM help? an empirical study on task-oriented dialog pre-training,” in *Proceedings of the Second Workshop on Insights from Negative Results in NLP*, Nov. 2021, pp. 54–61.
- [47] S. Lee, M. Kang, J. Lee, S. J. Hwang, and K. Kawaguchi, “Self-Distillation for Further Pre-training of Transformers,” in *ICLR*, 2023.
- [48] X. Chen and K. He, “Exploring Simple Siamese Representation Learning,” in *CVPR*, Jun 2021, pp. 15 745–15 753.
- [49] D. Niizumi, D. Takeuchi, Y. Ohishi, N. Harada, and K. Kashino, “BYOL for Audio: Self-Supervised Learning for General-Purpose Audio Representation,” in *IJCNN*, Jul 2021.
- [50] K. J. Piczak, “ESC: Dataset for Environmental Sound Classification,” in *ACM-MM*, 2015, pp. 1015–1018.
- [51] J. Salamon, C. Jacoby, and J. P. Bello, “A dataset and taxonomy for urban sound research,” in *ACM-MM*, 2014, pp. 1041–1044.
- [52] P. Warden, “Speech Commands: A Dataset for Limited-Vocabulary Speech Recognition,” *arXiv preprint arXiv:1804.03209*, Apr. 2018.
- [53] A. Nagrani, J. S. Chung, and A. Zisserman, “Voxceleb: A large-scale speaker identification dataset,” in *Interspeech*, 2017, pp. 2616–2620.

- [54] H. Cao, D. G. Cooper, M. K. Keutmann, R. C. Gur, A. Nenkova, and R. Verma, "CREMA-D: Crowd-sourced emotional multimodal actors dataset," *IEEE Trans. Affective Comput.*, vol. 5, no. 4, 2014.
- [55] G. Tzanetakis and P. Cook, "Musical genre classification of audio signals," *IEEE Speech Audio Process.*, vol. 10, no. 5, 2002.
- [56] J. Engel, C. Resnick, A. Roberts, S. Dieleman, M. Norouzi, D. Eck, and K. Simonyan, "Neural audio synthesis of musical notes with WaveNet autoencoders," in *ICML*, 2017.
- [57] J. Turian, J. Shier, G. Tzanetakis, K. McNally, and M. Henry, "One Billion Audio Sounds from GPU-enabled Modular Synthesis," in *DAFx2020*, 2021.
- [58] K. Koutini, J. Schlüter, H. Eghbal-zadeh, and G. Widmer, "Efficient Training of Audio Transformers with Patchout," *Interspeech*, pp. 2753–2757, 2022.
- [59] A. Kumar, R. Shen, S. Bubeck, and S. Gunasekar, "How to Fine-Tune Vision Models with SGD," *arXiv preprint arXiv:2211.09359*, 2022.
- [60] K. MacLean, "Voxforge", 2018, available at <http://www.voxforge.org/home>.
- [61] C. Kereliuk, B. L. Sturm, and J. Larsen, "Deep Learning and Music Adversaries," *IEEE Trans. Multimedia*, vol. 17, no. 11, p. 2059–2071, Nov 2015.
- [62] B. L. Sturm, "The GTZAN dataset: Its contents, its faults, their effects on evaluation, and its future use," *ArXiv*, vol. abs/1306.1461, 2013.
- [63] H. Zhang, M. Cisse, Y. N. Dauphin, and D. Lopez-Paz, "mixup: Beyond Empirical Risk Minimization," in *ICLR*, 2018.
- [64] I. Loshchilov and F. Hutter, "SGDR: Stochastic gradient descent with warm restarts," *ICLR*, 2017.
- [65] D. Niizumi, D. Takeuchi, Y. Ohishi, N. Harada, and K. Kashino, "Composing General Audio Representation by Fusing Multilayer Features of a Pre-trained Model," in *EUSIPCO*, 2022, pp. 200–204.
- [66] K. Chen, X. Du, B. Zhu, Z. Ma, T. Berg-Kirkpatrick, and S. Dubnov, "HTS-AT: A Hierarchical Token-Semantic Audio Transformer for Sound Classification and Detection," in *ICASSP*, 2022, pp. 646–650.
- [67] A. Gazneli, G. Zimmerman, T. Ridnik, G. Sharir, and A. Noy, "End-to-End Audio Strikes Back: Boosting Augmentations Towards An Efficient Audio Classification Network," *arXiv preprint arXiv:2204.11479*, 2022.
- [68] Q. Kong, Y. Cao, T. Iqbal, Y. Wang, W. Wang, and M. D. Plumbley, "PANNs: Large-Scale Pretrained Audio Neural Networks for Audio Pattern Recognition," *IEEE/ACM Trans. Audio, Speech, Language Process.*, vol. 28, pp. 2880–2894, 2020.
- [69] S. wen Yang, P.-H. Chi, Y.-S. Chuang, C.-I. J. Lai, K. Lakhotia, Y. Y. Lin, A. T. Liu, J. Shi, X. Chang, G.-T. Lin, T.-H. Huang, W.-C. Tseng, K. tik Lee, D.-R. Liu, Z. Huang, S. Dong, S.-W. Li, S. Watanabe, A. Mohamed, and H. yi Lee, "SUPERB: Speech Processing Universal PERformance Benchmark," in *Interspeech*, 2021, pp. 1194–1198.
- [70] V. Panayotov, G. Chen, D. Povey, and S. Khudanpur, "Librispeech: An ASR corpus based on public domain audio books," in *ICASSP*, 2015, pp. 5206–5210.
- [71] Y. Meng, H.-J. Chen, J. Shi, S. Watanabe, P. Garcia, H.-y. Lee, and H. Tang, "On Compressing Sequences for Self-Supervised Speech Models," in *SLT*, 2022, pp. 1128–1135.
- [72] B. M. Rocha, D. Filos, L. Mendes, G. Serbes, S. Ulukaya, Y. P. Kahya, N. Jakovljevic, T. L. Turukalo, I. M. Vogiatzis, E. Perantoni, E. Kaimakamis, P. Natsiavas, A. Oliveira, C. Jácome, A. Marques, N. Maglaveras, R. P. Paiva, I. Chouvarda, and P. de Carvalho, "An open access database for the evaluation of respiratory sound classification algorithms," *Physiological Measurement*, vol. 40, p. 035001, Mar 2019.
- [73] I. Moummad and N. Farugia, "Pretraining Respiratory Sound Representations using Metadata and Contrastive Learning," in *WASPAA*, 2023, pp. 1–5.
- [74] P. Khosla, P. Teterwak, C. Wang, A. Sarna, Y. Tian, P. Isola, A. Maschinot, C. Liu, and D. Krishnan, "Supervised Contrastive Learning," in *NeurIPS*, 2020, pp. 18 661–18 673.
- [75] E. Fonseca, X. Favory, J. Pons, F. Font, and X. Serra, "FSD50K: An Open Dataset of Human-Labeled Sound Events," *IEEE/ACM Trans. Audio, Speech, Language Process.*, vol. 30, pp. 829–852, 2022.
- [76] J. R. Hermans, G. Spanakis, and R. Möckel, "Accumulated gradient normalization," in *ACML*, vol. 77, Nov 2017, pp. 439–454.
- [77] S. Bae, J.-W. Kim, W.-Y. Cho, H. Baek, S. Son, B. Lee, C. Ha, K. Tae, S. Kim, and S.-Y. Yun, "Patch-Mix Contrastive Learning with Audio Spectrogram Transformer on Respiratory Sound Classification," in *Interspeech*, 2023, pp. 5436–5440.
- [78] Q. Zhang, J. Zhang, J. Yuan, H. Huang, Y. Zhang, B. Zhang, G. Lv, S. Lin, N. Wang, X. Liu, M. Tang, Y. Wang, H. Ma, L. Liu, S. Yuan, H. Zhou, J. Zhao, Y. Li, Y. Yin, L. Zhao, G. Wang, and Y. Lian, "SPRSound: Open-source sjtU paediatric respiratory sound database," *IEEE Trans. Biomed. Circuits Syst.*, vol. 16, no. 5, pp. 867–881, 2022.
- [79] A. C. Li, A. A. Efros, and D. Pathak, "Understanding Collapse in Non-Contrastive Siamese Representation Learning," in *ECCV*, 2022, p. 490–505.
- [80] J. Deng, W. Dong, R. Socher, L.-J. Li, K. Li, and L. Fei-Fei, "ImageNet: A large-scale hierarchical image database," in *CVPR*, 2009, pp. 248–255.



**Daisuke Niizumi** Daisuke Niizumi received the B.S. and M.S. degrees from the Department of Computer Science and Systems Engineering of the Kyushu Institute of Technology in 1995 and 1997, respectively. From 1997 to 2020, he was a senior software and machine learning engineer/manager at several consumer electronics companies. He joined NTT Corporation in 2020. His research interests include representation learning, self-supervised learning, and multimodal deep learning.



**Daiki Takeuchi** Daiki Takeuchi received the B.S. and M.S. degrees from the Department of Intermedia Art and Science of Waseda University in 2018 and 2020, respectively. He joined NTT Corporation in 2020. His research interests include signal processing and machine learning for multimodal information processing related to audio.



**Yasunori Ohishi** Yasunori Ohishi (M '12) received the Ph.D. degree from Nagoya University in 2009. Since joining NTT in 2009, he has been researching speech and audio signal processing. His research interests generally concern audio event detection, music information retrieval, and crossmodal learning with audio applications.



**Noboru Harada** Noboru Harada (M'99–SM'18) received the B.S. and M.S. degrees in computer science and systems engineering from the Kyushu Institute of Technology, Fukuoka, Japan, in 1995 and 1997, respectively, and the Ph.D. degree in computer science from the University of Tsukuba, Ibaraki, Japan, in 2017. He is currently a Senior Distinguished Researcher at Nippon Telegraph and Telephone Corporation and a visiting professor at Hokkaido University, Japan. Since joining NTT Corporation, Tokyo, Japan, in 1997, he has been

involved with research on speech and audio signal processing, such as high-efficiency coding, lossless compression, and acoustic event detection, including anomaly sound detection.



**Kunio Kashino** Kunio Kashino (SM '05) received the Ph.D. degree from the University of Tokyo in 1995. He is currently a Fellow at Nippon Telegraph and Telephone Corporation and a visiting professor at Osaka University and the National Institute of Informatics, Japan. His research interests include audio and crossmodal information processing, media search, and biomedical informatics. He is a member of Association for Computing Machinery (ACM) and a Fellow of the Institute of Electronics, Information and Communication Engineers (IEICE). He

received the IEEE Transactions on Multimedia Paper Award in 2004, the Maejima Award in 2010, the Kenjiro Takayanagi Achievement Award in 2016, the IEICE Achievement Award in 2002 and 2017, and the Commendation for Science and Technology by the Minister of Education, Culture, Sports, Science and Technology in 2019.